ALERT-GEOMATERIALS SCHOOL 2015
Aussois (Fr), October 1 - 3

UNIVERSITÀ DEGLI STUDI DI PADOVA

Finite element analysis of non-isothermal multiphase porous media in dynamics, with application to strain localisation simulation

Lorenzo Sanavia[1], **Toan Duc Cao**[1,2]

[1]University of Padova, Italy - lorenzo.sanavia@unipd.it
[2]Technische Universitaet Darmstadt, Germany

MUMOLADE

MARIE CURIE ACTIONS

Thanks also to: Maria Lazari[1], Mareva Passarotto[1], Bernhard Schrefler[1]

Outline:

- Motivations: Geo-environmental and Energy engineering problems
- Mathematical model (thermodynamically consistent mechanistic theory – Hybrid Mixture Theory): governing equations, constitutive models, i.c. & b.c.
- Finite Element discretisation
- Numerical validation and simulation of strain localisation in dense sand

This lecture aims to:

- Show development of a **fully coupled finite element model** for non-isothermal non-linear multiphase elasto-plastic porous continuum in dynamics (THM fem model).

- Validation (comparison with analytical solutions or more approximated numerical solutions)

- Strain localisation analysis (localised failure of…. geomaterials)

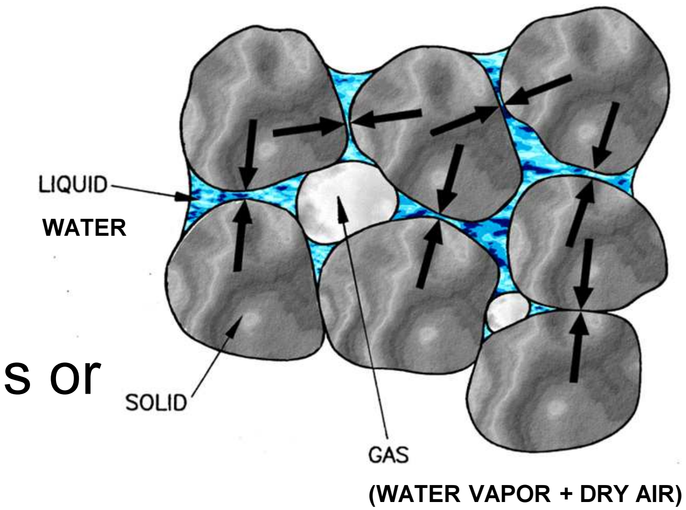

Microscopic view of three-phase geomaterial (soil, concrete, rocks)

Motivation: catastrophic landslides

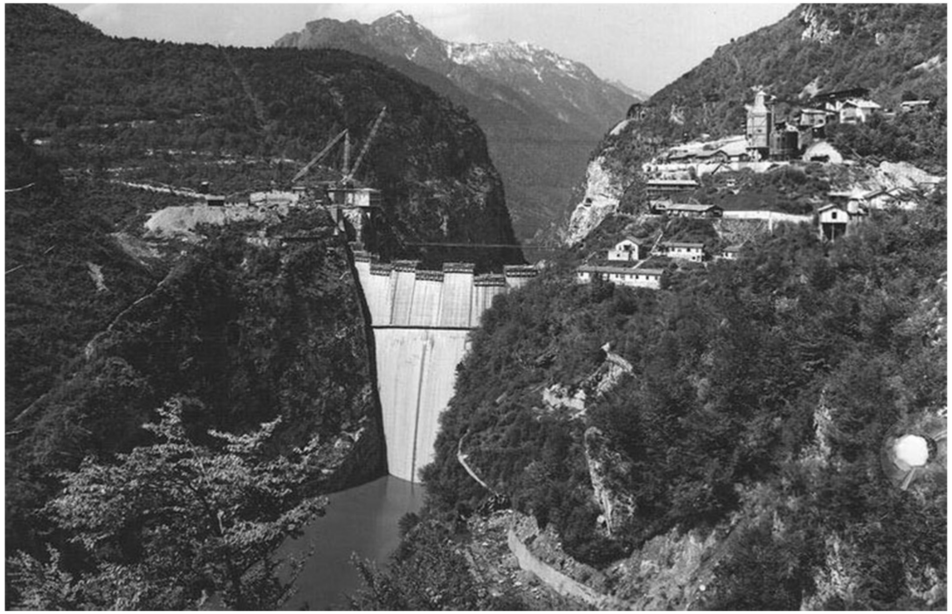

Vajont, Italy, October 9, 1963

- Dam 263.5 m tall (462 - 725,50 m slm - tallest in world)
- Reservoir contained ~ 170 million m^3 of water
- Reservoir filling + heavy rainfall + high water pressure load from the bedrock ⇨ reactivation of a **prehistoric** slide

Motivation: catastrophic landslides

Vajont, Italy, October 9, 1963

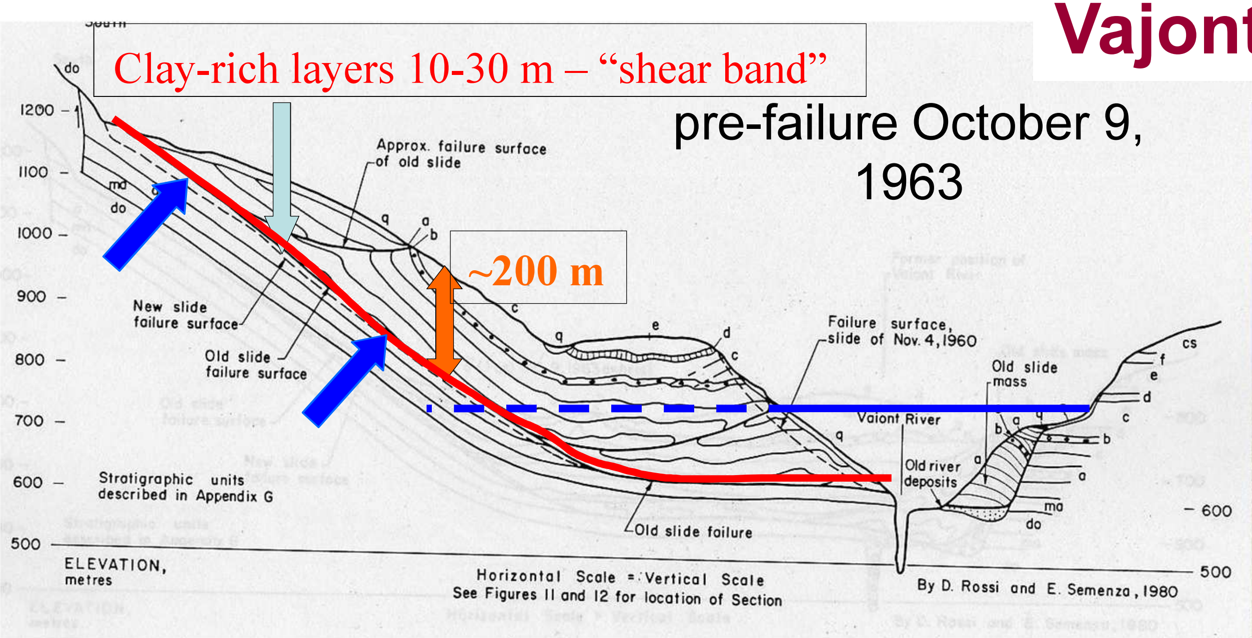

(Rossi and Semenza, 1980)

- Reactivation of a prehistoric slide:

  270 million m^3 of rock - 200-250 m thick mass of rock

  slide moved in 20-25 s - velocity 20-30 m/s;

  water wave ~ 210 m above top of dam ⇨ *2043 persons died*

Motivation: catastrophic landslides

• Onset of landslide: increase of temperature in the failure zone (friction-generated thermal effects) ⇨ increase of water pressure and loss of clay strength ⇨ vapour cushion of zero friction may have appeared, increasing the slide velocity *(Hendron and Patton 1985; Vardoulakis 2002; Cecinato 2011; …)*

• "Ingredients" for modelling: non-isothermal multiphase porous media, dynamics, frictional heating, large strains.

963

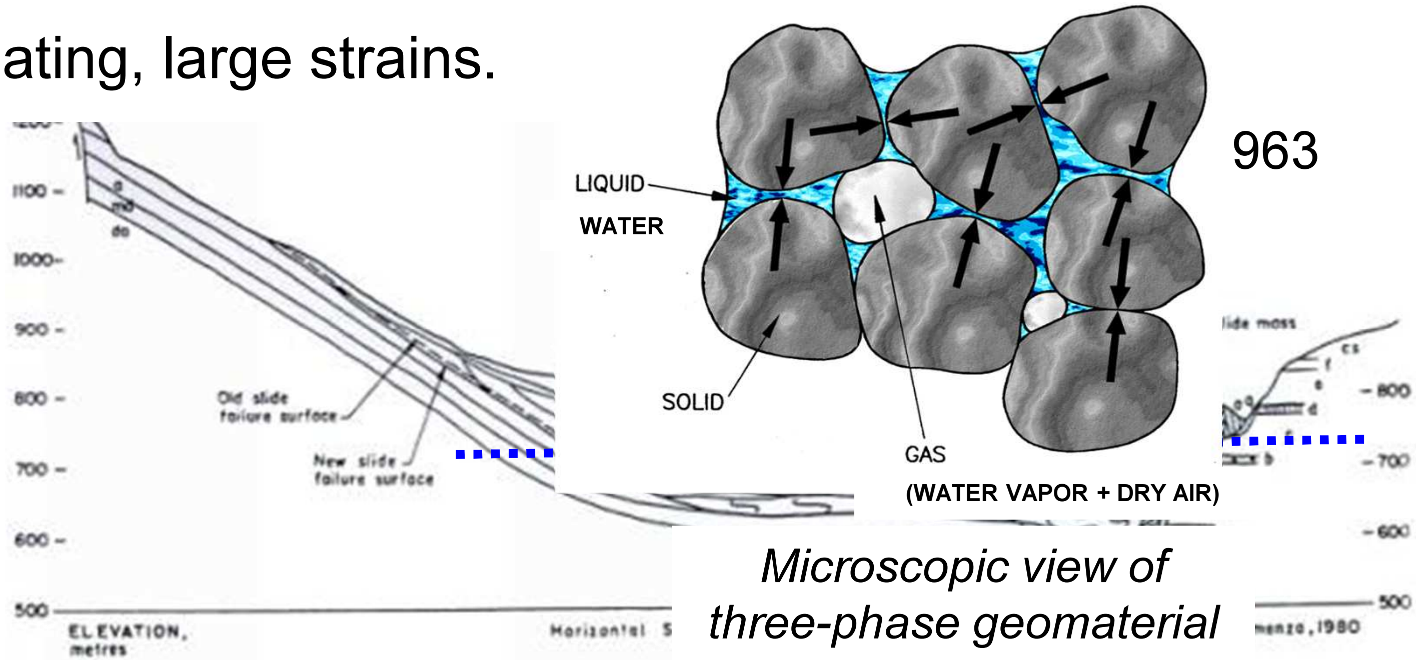

Microscopic view of three-phase geomaterial (soil, concrete, rocks)

Motivation: seismic behaviour of deep nuclear waste disposal

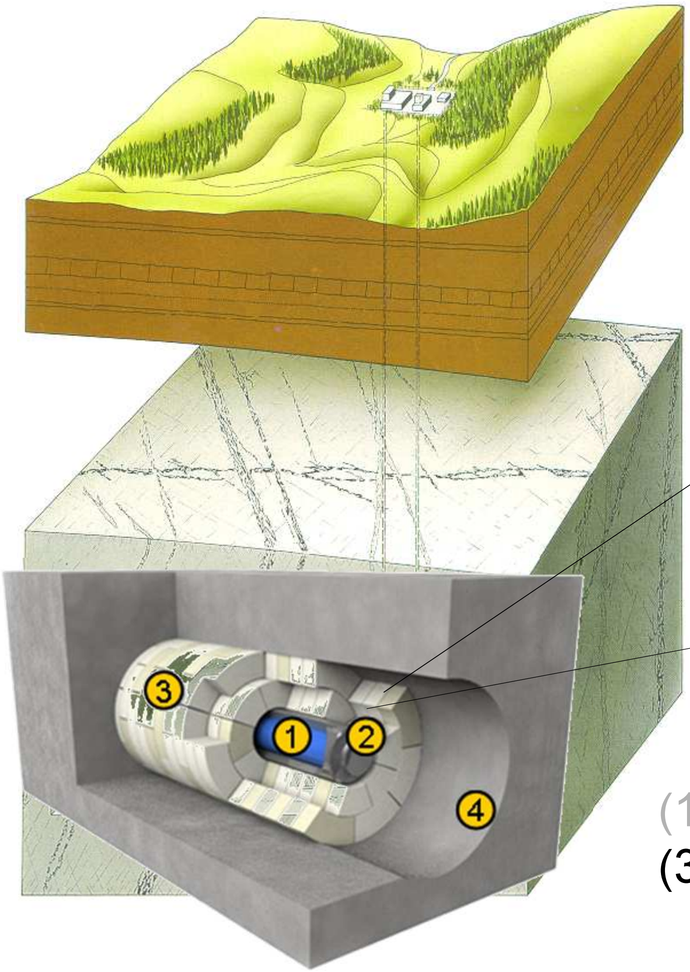

buffer and host material: composed by a solid skeleton with open pores containing one or more fluids loaded with heat generated by the waste

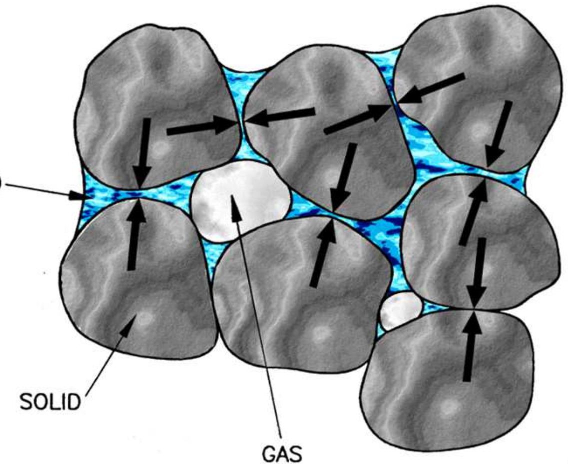

Microscopic view (partially saturated soil)

(deep: -400 m, -700 m)

(1) vitrified waste, (2) steel canister,
(3) buffer material, (4) host material

Typical scheme of a deep geological repository for nuclear waste
(*Gens, Olivella, CISM lecture notes 2001*)

Motivation: oil sands production

Bituminous sands, colloquially known as oil sands or tar sands, are a *type of unconventional petroleum deposit*. The sands
contain naturally occurring mixtures of sand, clay, water, and a dense and e red
to as bitumen (or colloquially "tar" due to its similar appearance, odour, rge
amounts in many countries throughout the world, but are found in extremely

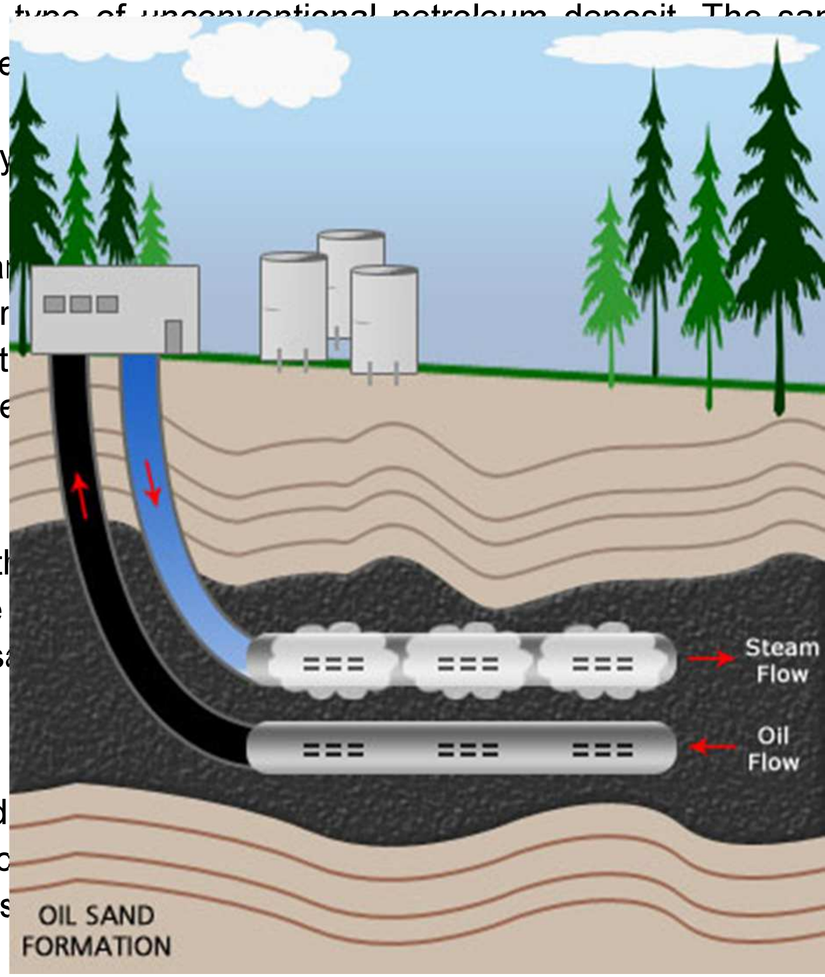

The crude bitumen contained in the Canadian oil sands is described by Ca mi-
solid or solid phase in natural deposits. Bitumen is a thick, sticky form of cr ow
unless heated or diluted with lighter hydrocarbons. At room temperature, it ies
often refer to similar types of crude oil as extra-heavy oil, because Venezue ess
viscous, allowing it to flow more easily.

Oil sands reserves have only recently been considered to be part of th ew
technology enable them to be profitably extracted and upgraded to usable nal
oil or crude bitumen, in order to distinguish the bitumen extracted from oil s wn
as crude oil traditionally produced from oil wells.

Making liquid fuels from oil sands requires energy for steam injection and the
amount of greenhouse gases per barrel of final product as the "produc nal
products is included, the so-called "Well to Wheels" approach, oil sands ore
greenhouse gases than conventional crude.[4]

… **the oil made to flow into wells by in situ techniques, which reduce the viscosity by injecting steam, solvents, and/or hot air into the sands**. These processes can use more water and require larger amounts of energy than conventional oil extraction, although many conventional oil fields also require large amounts of water and energy to achieve good rates of production.

http://www.cbc.ca/blueprintalberta/features/oilsands.html

Motivation: Hydraulic fracturing (1947)

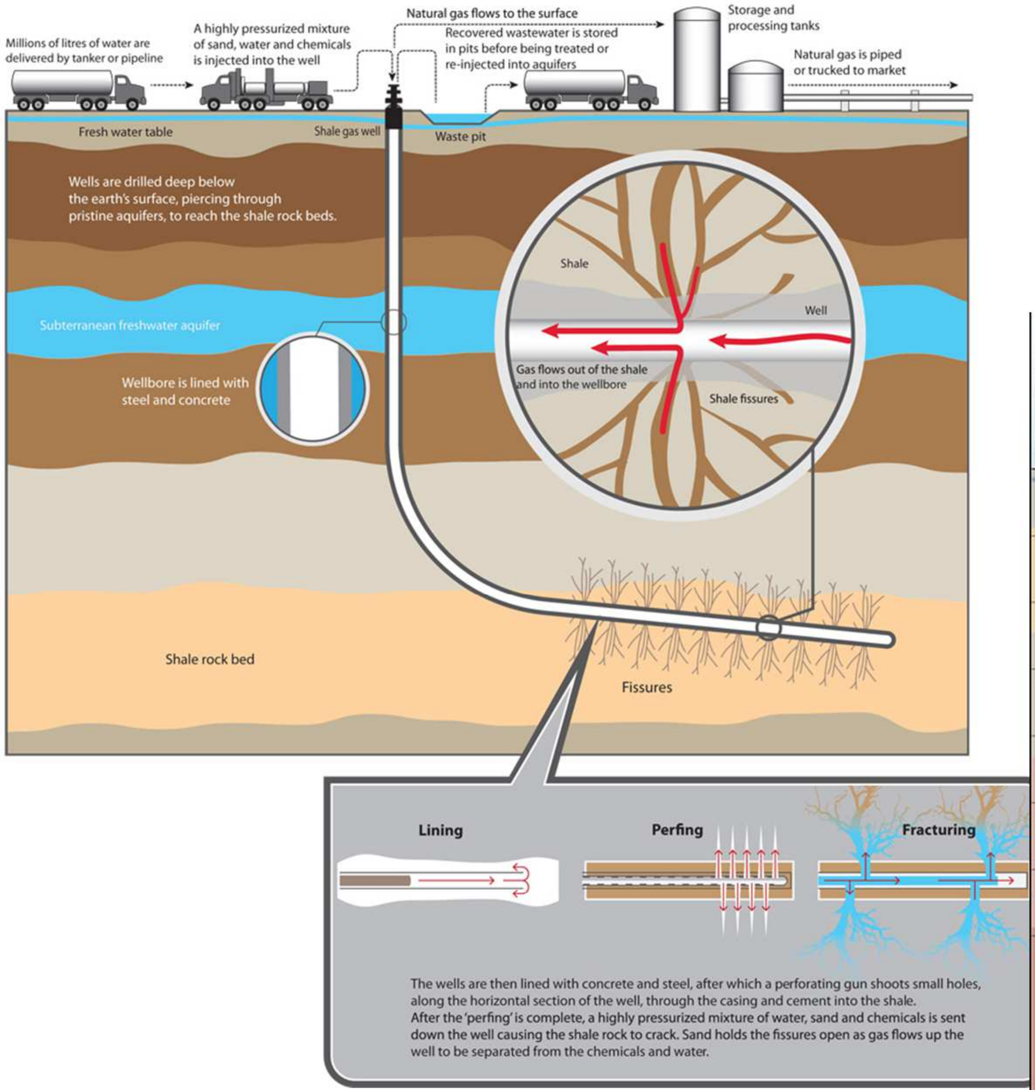

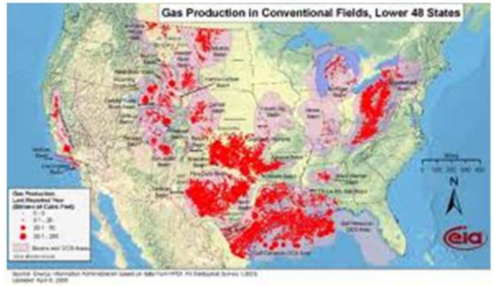

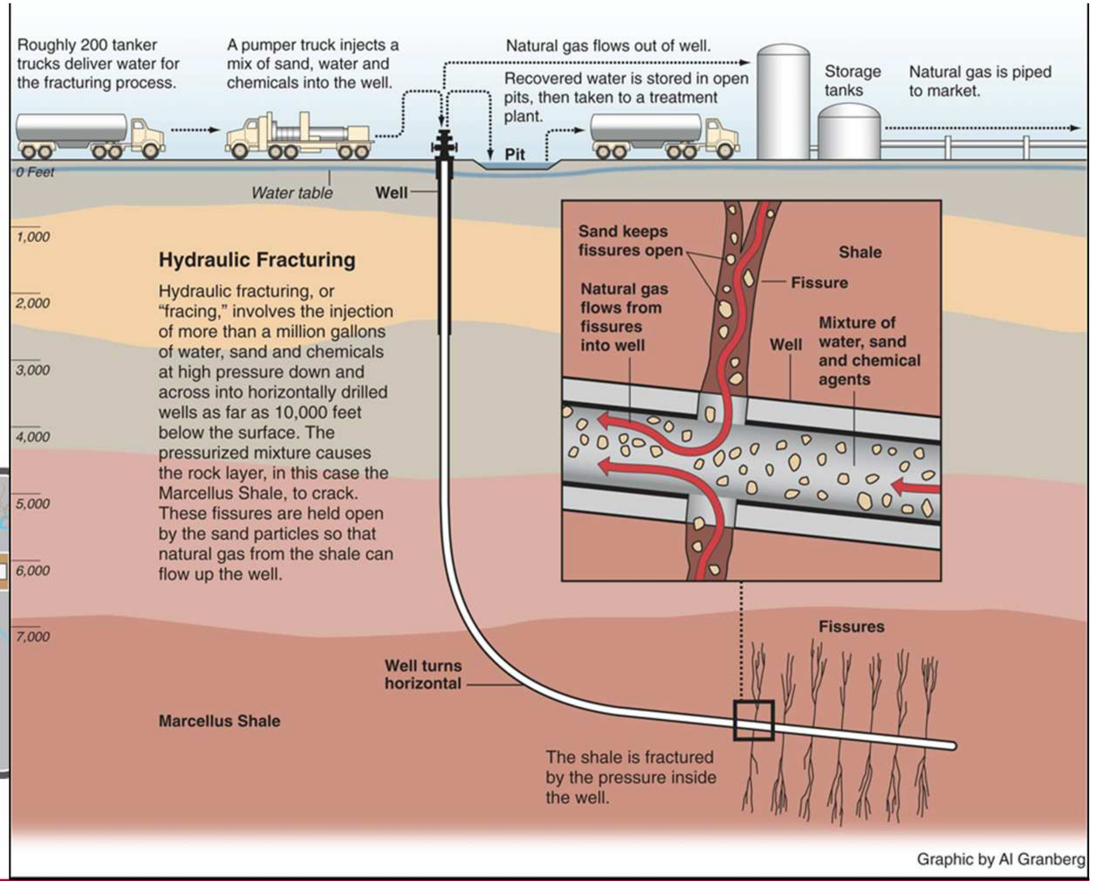

Mathematical model

liquid phase
(liquid water)

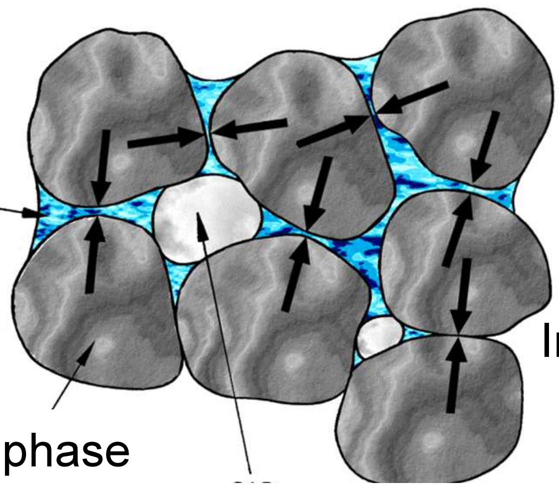

Microscopic view of a three-phase material

Intergranular forces due to capillary effects

solid phase

gas phase (dry air and/or water vapour)

Mechanics of non-isothermal multiphase porous materials:

- Balance equations
- Generalised effective stress principle
- THM constitutive models (dependent on temperature and capillary pressure)

State of art - porous media models in dynamics

1980: O.C. Zienkiewicz , C.T. Chang, P. Bettes, Géotechnique
1983: **A.H. Chan,** PhD Thesis, Swansea University. *Isothermal models.*

1990: O.C. Zienkiewicz, A.H.C. Chan, M. Pastor, D.K. Paul, T. Shiomi, PRSA
Isothermal 3-phase formulation with air phase assumption
1995: E.A. Meroi, B.A. Schrefler, O.C. Zienkiewicz, NAG.
Isothermal 3-phase formulation with air phase assumption.

1998: R.W. Lewis, B.A. Schrefler "The Finite Element Method in the Static and Dynamic Deformation and Consolidation of Porous Media", Wiley, 1998.
Non-isothermal dynamic 3-phase formulation, non-isothermal 3-phase quasi-static implementation.

1998: B.A. Schrefler, R. Scotta, CMAME, 1998. *Isothermal 3-phase formulation and implementation.*

1999: O.C. Zienkiewicz, A. Chan, M. Pastor, B.A. Schrefler, T. Shiomi "Computational Geomechanics with special reference to earthquake engineering", Wiley, 1999.
Isothermal 3-phase dynamic formulation and implementation with air phase assumption.

2009: **N. Ravichandran, K.K. Muraleetharan**, IJNAMG, " Dynamics of unsaturated soils using various finite element formulations". *Isothermal 3-phase dynamic formulation.*

2010: B. Markert "Dynamic wave propagation in infinite saturated porous media half spaces", Habilitation thesis, Universitaet Stuttgart. *Isothermal 2-phase dynamic formulation and implementation.*

State of art - porous media models in dynamics

2010: B. Albers “Modeling and numerical analysis of wave propagation in saturated and partially saturated porous media”, Habilitation thesis, Technische Universitaet Berlin.

Isothermal 3-phase dynamics formulation.

2010: **M. Nenning and M. Schanz**, IJNAMG, “Infinite elements in a poroelastodynamics”.

Isothermal, wave propagation problems in unbounded saturated porous media.

2011: A.R Khoei, T. Mohammadnejad, Computers and Geotechnics, “Numerical modeling of multiphase fluid flow in deforming porous media: a comparison between two- and three-phase models for seismic analysis of earth and rockfill dams” . *Isothermal model, 2- and 3-phase formulation.*

2012: Y. Heider, Ph.D thesis, “Saturated Porous Media Dynamics with Application to Earthquake Engineering”, Universitaet Stuttgart. *Isothermal 3-phase formulation with application to strain localisation simulation*.

2013: I.D. Moldovan, T.D. Cao and J.A. Teixeira de Freitas, IJNME, “Elastic wave propagation in unsaturated porous media using hybrid-Trefftz stress elements”.

Isothermal 3-phase formulation, modeling for shock wave propagation in porous media.

… … …

THM implementation in dynamics: not yet published

Mathematical model

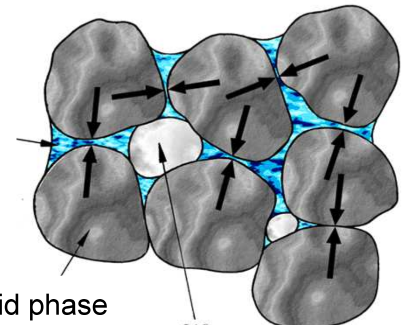

based on: ***Hybrid Mixture theory***

Lewis and Schrefler '98, The finite element method in the static and dynamic ...,

Hassanizadeh and Gray AWR 1979, 1980, 1990

Schrefler AMR 2002

*Thermodynamically Constrained Averaging Theory (**TCAT**): Gray and Miller, 2005, … …; Gray and Schrefler, 2007; Gray et al., 2012*

Assumptions (THM model):

- local thermodynamic equilibrium state
- constituents microscopically non-polar
- immiscible constituents (except dry air and water vapour)
- water vapour, dry air and their mixture: perfect gases
- phase change for liquid water and its vapour (evaporation/condensation – adsorption/desorption)
- small strains (for the implement model)

Hybrid mixture theory

Microscopic balance equations

Spatial averaging operators (*Hassanizadeh and Gray AWR 1979, 1980, 1990*)

Macroscopic balance equations

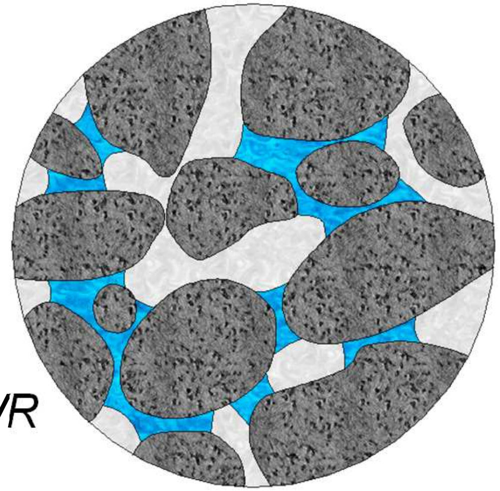

Microscopic view

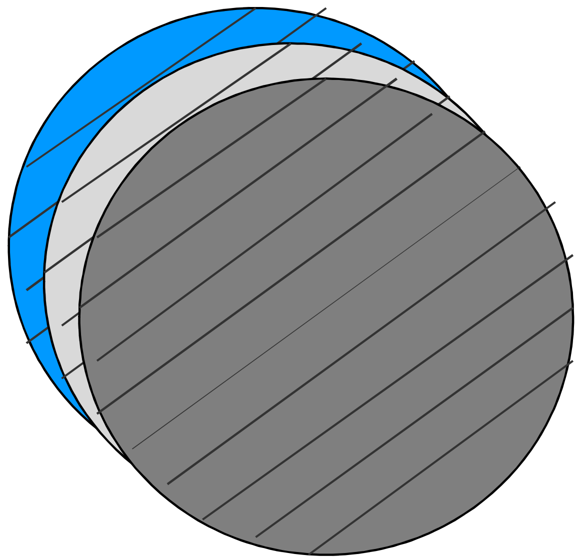

macroscopic view of averaged continuum

- As a results a substitute continua which fill the entire domain simultaneously is obtained, instead of the real fluids and solid, which fill only a part of it.
- These substitute continua has a reduced density, which is obtained through the volume fraction $\eta^{\pi}(x,t) = dv^{\pi}(\mathbf{x},t) / dv(\mathbf{x},t)$.

Macroscopic balance equations

(Lewis and Schrefler '98)

Linear momentum balance equations of the mixture:

$$div\left(\boldsymbol{\sigma}' - \mathbf{I}\alpha\left[p^g - S_w p^c\right]\right) + \rho\mathbf{g} - \rho\mathbf{a}^s - nS_w\rho^w\left[\mathbf{a}^{ws} + \mathbf{v}^{ws}\cdot\nabla\mathbf{v}^w\right] - nS_g\rho^g\left[\mathbf{a}^{gs} + \mathbf{v}^{gs}\cdot\nabla\mathbf{v}^g\right] = \mathbf{0}$$

Enthalpy balance equation of the mixture:

$$\begin{aligned}
&\left[C_p^w nS_w\rho^w \frac{k^{rw}\mathbf{k}_w}{\mu^w}\left[-grad\,p^w + \rho^w\left(\mathbf{g} - \mathbf{a}^s - \mathbf{a}^{ws}\right)\right] + C_p^g nS_g\rho^g \frac{k^{rg}\mathbf{k}_g}{\mu^g}\left[-grad\,p^g + \rho^g\left[\mathbf{g} - \mathbf{a}^s - \mathbf{a}^{gs}\right]\right]\right]\cdot grad\,T + \\
&+\left(\rho C_p\right)_{eff}\dot{T} - div\left(\chi_{eff}\,grad\,T\right) - \rho^w\left[\frac{\alpha-n}{K_s}S_w^2 + \frac{nS_w}{K_w}\right]\Delta H_{vap}\dot{p}^w - \rho^w\frac{\alpha-n}{K_s}S_wS_g\Delta H_{vap}\dot{p}^g - \Delta H_{vap}\rho^w S_w\alpha\,\mathbf{mL}\dot{\mathbf{u}} + \\
&+\Delta H_{vap}\beta_{sw}\dot{T} - \left[\rho^w\left[\frac{\alpha-n}{K_s}p^wS_w - \frac{\alpha-n}{K_s}p^gS_w + n\right] - \rho^{gw}\left[\frac{\alpha-n}{K_s}p^cS_g + n\right]\right]\Delta H_{vap}\dot{S}_w + \\
&-div\left(\rho^w\frac{k^{rw}\mathbf{k}_w}{\mu^w}\left[-grad\,p^w + \rho^w\left(\mathbf{g} - \mathbf{a}^s - \mathbf{a}^{ws}\right)\right]\right)\Delta H_{vap} = 0
\end{aligned}$$

Macroscopic balance equations

(Lewis and Schrefler '98)

Liquid species mass balance equation (solid, liquid water & vapour):

$$\left[\rho^w\left[\frac{\alpha-n}{K_s}S_w^2+\frac{nS_w}{K_w}\right]+\rho^{gw}\frac{\alpha-n}{K_s}S_wS_g\right]\dot{p}^w+\rho^w\frac{\alpha-n}{K_s}S_wS_g\dot{p}^{gw}+\rho^{gw}\frac{\alpha-n}{K_s}S_g^2\dot{p}^{gw}+\left[\rho^wS_w+\rho^{gw}S_g\right]\alpha\, div\mathbf{v}^s+$$

$$-\left[\rho^w\beta_{sw}+\rho^{gw}\beta_s[\alpha-n]S_g\right]\dot{T}+nS_g\dot{\rho}^{gw}+div\mathbf{J}_g^{gw}+\left[\rho^w\left[\frac{\alpha-n}{K_s}p^wS_w-\frac{\alpha-n}{K_s}p^gS_w+n\right]-\rho^{gw}\left[\frac{\alpha-n}{K_s}p^cS_g+n\right]\right]\dot{S}_w+$$

$$+div\left(\rho^w\frac{k^{rw}\mathbf{k}}{\mu^w}\left[-gradp^w+\rho^w\left[\mathbf{g}-\mathbf{a}^s-\mathbf{a}^{ws}\right]\right]\right)+div\left(\rho^{gw}\frac{k^{rgw}\mathbf{k}}{\mu^{gw}}\left[-gradp^{gw}+\rho^{gw}\left[\mathbf{g}-\mathbf{a}^s-\mathbf{a}^{gws}\right]\right]\right)=0$$

Dry air mass balance equation:

$$\frac{\alpha-n}{K_s}S_wS_g\dot{p}^w+\frac{\alpha-n}{K_s}S_g^2\dot{p}^{ga}+\alpha S_g div\,\mathbf{v}^s+\frac{nS_g}{\rho^{ga}}\dot{\rho}^{ga}+\frac{1}{\rho^{ga}}div\,\mathbf{J}_g^{ga}+$$

$$-\left[\frac{\alpha-n}{K_s}p^cS_g+n\right]\dot{S}_w-\beta_s(\alpha-n)S_g\dot{T}+\frac{1}{\rho^{ga}}div\left(\rho^{ga}\frac{k^{rg}\mathbf{k}_g}{\mu^g}\left[-gradp^g+\rho^g\left[\mathbf{g}-\mathbf{a}^s-\mathbf{a}^{gs}\right]\right]\right)=0$$

Macroscopic balance equations (implemented model)

Assumption: when relative acceleration of the fluids and convective terms can be neglected

$$\left[\mathbf{a}^{ws} + \mathbf{v}^{ws} \cdot \nabla \mathbf{v}^{w}\right]; \qquad \left[\mathbf{a}^{gs} + \mathbf{v}^{gs} \cdot \nabla \mathbf{v}^{g}\right]$$

$\mathbf{u}$-p **form** *(A.H. Chan,1983, PhD Thesis, Swansea University)*

(Zienkiewicz O.C., Chan A.H., Pastor M., Schrefler B.A., Shiomi T., Wiley, 1999)

(Valid for low frequencies problems, e.g. in earthquake engineering)

- $\mathbf{u}$-p-T **form**

State variables: (measurable)

p^c capillary pressure

p^g gas pressure

T temperature

$\boldsymbol{u}$ solid displacements

$p^w = p^g - p^c$

approximated in dynamics

(e.g Hassanizadeh et al. VZJ 2002)

Validity of u-p form

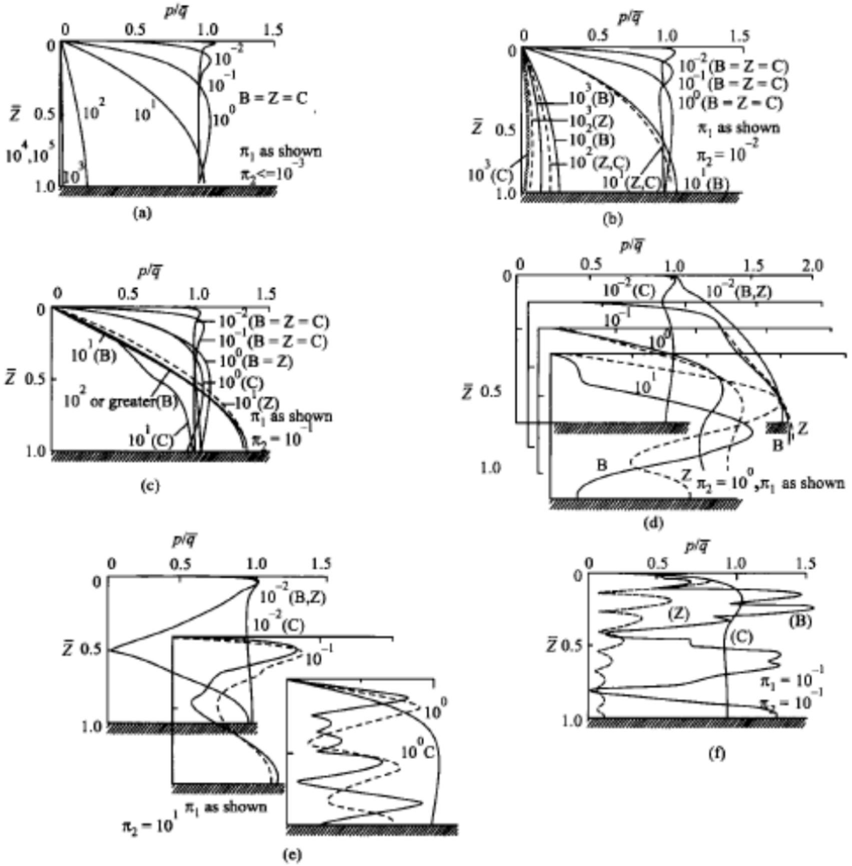

Figure 2.1 The soil column — variation of pore pressure with depth for various values of π_1 and π_2 ——— B (Biot theory) - - - - z (u-p approximation theory) ▬ c (Consolidation theory) (Solution (C) is independent of π_2). Reproduced from Zienkiewicz (1980) by permission of the Institution of Civil Engineers

$$\pi_1 = \frac{kV_c^2}{g\beta\omega L^2} = \left(\frac{2}{\beta\pi}\right)\frac{k}{g}\frac{T}{\hat{T}} \qquad \kappa = \frac{k_f/n}{D + k_f/n} = 0.973$$

$$\pi_2 = \frac{\omega^2 L^2}{V_c^2} = \pi^2\left(\frac{T}{\hat{T}}\right)^2 \qquad n = \beta = 0.333$$

$$\bar{z} = z/L$$

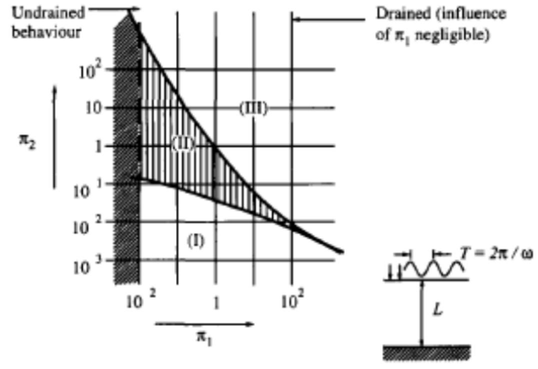

Figure 2.2 Zones of sufficient accuracy for various approximations: Zone 1, B = Z = C, slow phenomena ($\ddot{w}$ and $\ddot{u}$ can be neglected) Zone 2, B = Z ≠ C, moderate speed ($\ddot{w}$ can be neglected) Zone III B ≠ Z ≠ C, fast phenomena ($\ddot{w}$ cannot be neglected only full Biot equation valid). Definition as in Figure 2.1. Reproduced from Zienkiewicz (1980) by permission of the Institution of Civil Engineers

$\pi_1 = k\rho V_c^2/\omega L^2 = 2k\rho_T/\pi\hat{T}^2$

$\pi_2 = \omega^2 L^2/V_c^2 = \pi^2(\frac{\hat{T}}{T})^2$

k=$\hat{k}/\rho g$, $\hat{k}$ – kinematic permeability, $\hat{T} = 2L/V_c$, $V_c^2 = (D + k_f/n)/\rho \sim \beta k_f/\rho_1 n \sim k_f/\rho_1$ (speed of sound in water), $\beta = \rho_f/\rho$, $n \sim 0.33$, $\beta \sim 0.33$

and Π_1 is dependent on the permeability k with the range defined by

$$0.97k' < \Pi_1 < 97k'$$

According to Figure 2.2 we can, with reasonable confidence:

(i) assume fully undrained behaviour when $\Pi_1 = 97k' < 10^{-2}$ or the permeability $k' < 10^{-4}$ m/s. (This is a very low value inapplicable for most materials used in dam construction).

(ii) We can assume **u**–p approximation as being valid when $k' < 10^{-3}$ m/s to reproduce the complete frequency range. However, when $k' < 10^{-1}$ m/s periods of less then 0.5 s are still well modelled.

We shall, therefore, typically use the **u**–p formulation appropriately in what follows reserving the full form for explicit transients where shocks and very high frequency are involved.

O.C. Zienkiewicz, A. Chan, M. Pastor, B.A. Schrefler, T. Shiomi "Computational Geomechanics with special reference to earthquake engineering", Wiley, 1999.

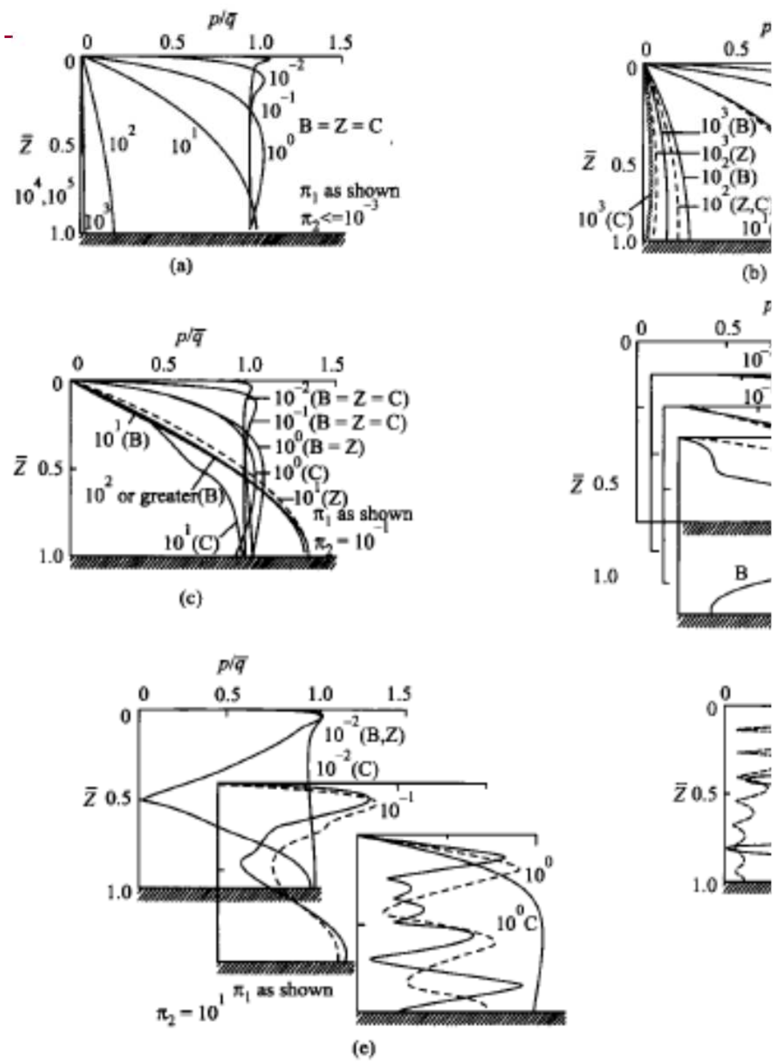

Figure 2.1 The soil column — variation of pore pressure with depth for
π_2 ———— B (Biot theory) - - - - z (u-p approximation theory)
theory) (Solution (C) is independent of π_2). Reproduced from Zienkiewi
of the Institution of Civil Engineers

$$\pi_1 = \frac{kV_c^2}{g\beta\omega L^2} = \left(\frac{2}{\beta\pi}\right)\frac{k}{g}\frac{T}{\hat{T}} \qquad \kappa = \frac{k_f/n}{D + k_f/n} = 0.973$$

$$\pi_2 = \frac{\omega^2 L^2}{V_c^2} = \pi^2\left(\frac{T}{\hat{T}}\right)^2 \qquad n = \beta = 0.333$$

$$\bar{z} = z/L$$

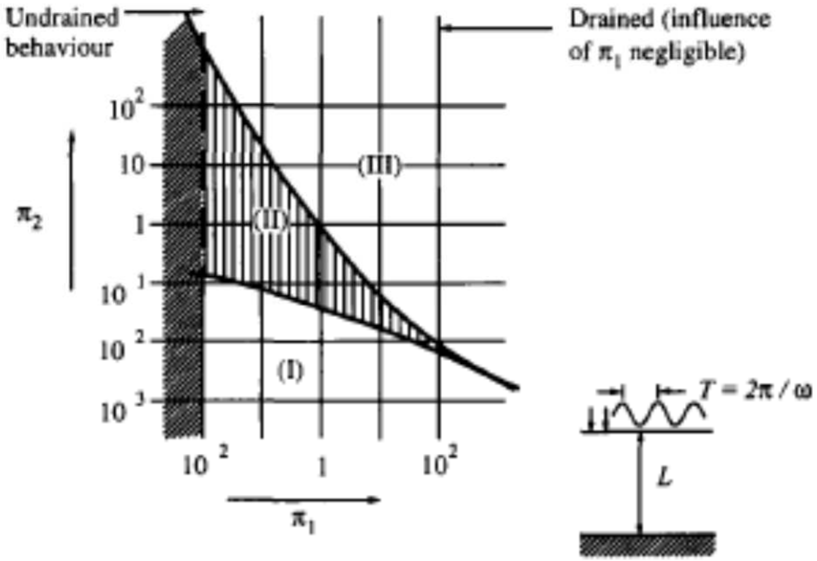

Figure 2.2 Zones of sufficient accuracy for various approximations: Zone 1, B = Z = C, slow phenomena ($\ddot{w}$ and $\ddot{u}$ can be neglected) Zone 2, B = Z ≠ C, moderate speed ($\ddot{w}$ can be neglected) Zone III B ≠ Z ≠ C, fast phenomena ($\ddot{w}$ cannot be neglected only full Biot equation valid). Definition as in Figure 2.1. Reproduced from Zienkiewicz (1980) by permission of the Institution of Civil Engineers

$\pi_1 = k\rho V_c^2/\omega L^2 = 2k\rho_T/\pi\hat{T}^2$

$\pi_2 = \omega^2 L^2/V_c^2 = \pi^2(\frac{\hat{T}}{T})^2$

k=$\hat{k}/\rho g$, $\hat{k}$ – kinematic permeability, $\hat{T} = 2L/V_c$, $V_c^2 = (D + k_f/n)/\rho \sim \beta k_f/\rho_1 n \sim k_f/\rho_1$ (speed of sound in water), $\beta = \rho_f/\rho$, $n \sim 0.33$, $\beta \sim 0.33$

and Π_1 is dependent on the permeability k with the range defined by

$$0.97k' < \Pi_1 < 97k'$$

According to Figure 2.2 we can, with reasonable confidence:

(i) assume fully undrained behaviour when $\Pi_1 = 97k' < 10^{-2}$ or the permeability $k' < 10^{-4}$ m/s. (This is a very low value inapplicable for most materials used in dam construction).

(ii) We can assume **u**–p approximation as being valid when $k' < 10^{-3}$ m/s to reproduce the complete frequency range. However, when $k' < 10^{-1}$ m/s periods of less then 0.5 s are still well modelled.

We shall, therefore, typically use the **u**–p formulation appropriately in what follows reserving the full form for explicit transients where shocks and very high frequency are involved.

Macroscopic balance equations (implemented model)

Additional assumptions:

- Incompressible solid grain at microscopic level:

$$K_s = \infty$$

$$\left(\alpha_{\text{Biot}} = 1 - \frac{K_T}{K_s}; \text{ for soils, } \alpha_{\text{Biot}} = 1 \right)$$

- Negligible: dynamic seepage forcing terms: solid acceleration $\mathbf{a}^s$ is neglected in mass balance equations (very small contribution compared with other terms - *A.H. Chan,1983, PhD Thesis , Swansea University* – isothermal conditions)

  and in enthalpy balance equation

Macroscopic balance equations (implemented model)

Linear momentum balance equations of the mixture:

$$div\left(\underbrace{\boldsymbol{\sigma}'-\left[p^g - S_w p^c\right]\mathbf{I}}\right)+\rho\mathbf{g}\boxed{-\rho\mathbf{a}^s}=\mathbf{0}$$

(thermodynamically consistent: *Schrefler 1984; Lewis & Schrefler 1987; Gray & Hassanizadeh 1991; Borja 2004*)

Enthalpy balance equation of the mixture:

$$\left[C_p^w n S_w \rho^w \frac{k^{rw}\mathbf{k}_w}{\mu^w}\left[-grad\left(p^g-p^c\right)+\rho^w\mathbf{g}\right]+C_p^g n S_g \rho^g \frac{k^{rg}\mathbf{k}_g}{\mu^g}\left[-grad p^g+\rho^g\mathbf{g}\right]\right]\cdot grad\,T$$

$$+\left(\rho C_p\right)_{eff}\dot{T}-div\left(\chi_{eff}\,grad\,T\right)\boxed{-\rho^w\frac{nS_w}{K_w}\Delta H_{vap}\left[\dot{p}^g-\dot{p}^c\right]-}\Delta H_{vap}\rho^w S_w \alpha\,\mathbf{mL}\dot{\mathbf{u}}$$

$$+\Delta H_{vap}\beta_{sw}\dot{T}-n\Delta H_{vap}\dot{S}_w\left[\rho^w-\rho^{gw}\right]-div\left(\rho^w\frac{k^{rw}\mathbf{k}_w}{\mu^w}\left[-grad p^w+\rho^w\mathbf{g}\right]\right)\Delta H_{vap}=\boldsymbol{\sigma}'\dot{\boldsymbol{\varepsilon}}^p$$

Macroscopic balance equations (implemented model)

Liquid species mass balance equation:

$$\boxed{\rho^w \frac{nS_w}{K_w}\left[\dot{p}^g - \dot{p}^c\right]} + \left[\rho^w S_w + \rho^{gw} S_g\right]\alpha\, div\mathbf{v}^s - \left[\rho^w \beta_{sw} + \rho^{gw}\beta_s[1-n]S_g\right]\dot{T} + nS_g\dot{\rho}^{gw}$$

$$+ div\mathbf{J}_g^{gw} + n\left[\rho^w - \rho^{gw}\right]\dot{S}_w + div\left(\rho^w \frac{k^{rw}\mathbf{k}_w}{\mu^w}\left[-grad\left(p^g - p^c\right) + \rho^w\mathbf{g}\right]\right) +$$

$$+ div\left(\rho^{gw}\frac{k^{rgw}\mathbf{k}_g}{\mu^{gw}}\left[-gradp^{gw} + \rho^{gw}\mathbf{g}\right]\right) = 0$$

Dry air mass balance equation:

$$\alpha S_g div\mathbf{v}^s + \frac{nS_g}{\rho^{ga}}\dot{\rho}^{ga} + \frac{1}{\rho^{ga}} div\mathbf{J}_g^{ga} - n\dot{S}_w +$$

$$+ \frac{1}{\rho^{ga}} div\left(\rho^{ga}\frac{k^{rg}\mathbf{k}_g}{\mu^g}\left[-gradp^g + \rho^g\mathbf{g}\right]\right) - \beta_s[1-n]S_g\dot{T} = 0$$

Coupled balance equations (model implemented)

1) $$div\left(\boldsymbol{\sigma}-\left[p^g-S_w p^c\right]\mathbf{I}\right)+\rho\mathbf{g}-\rho\mathbf{a}^s=\mathbf{0}$$ LMBE

2) $$\rho^w\frac{nS_w}{K_w}\left[\dot{p}^g-\dot{p}^c\right]+\left[\rho^w S_w+\rho^{gw}S_g\right]\alpha div\mathbf{v}^s-\left[\rho^w\beta_{sw}+\rho^{gw}\beta_s\left[1-n\right]S_g\right]\dot{T}+nS_g\dot{\rho}^{gw}$$
$$+div\mathbf{J}_g^{gw}+n\left[\rho^w-\rho^{gw}\right]\dot{S}_w+div\left(\rho^w\frac{k^{rw}\mathbf{k}_w}{\mu^w}\left[-grad\left(p^g-p^c\right)+\rho^w\mathbf{g}\right]\right)+$$
$$+div\left(\rho^{gw}\frac{k^{rgw}\mathbf{k}_g}{\mu^{gw}}\left[-grad p^{gw}+\rho^{gw}\mathbf{g}\right]\right)=0$$ wsMBE

3) $$\alpha S_g div\mathbf{v}^s+\frac{nS_g}{\rho^{ga}}\dot{\rho}^{ga}+\frac{1}{\rho^{ga}}div\mathbf{J}_g^{ga}-n\dot{S}_w+$$
$$+\frac{1}{\rho^{ga}}div\left(\rho^{ga}\frac{k^{rg}\mathbf{k}_g}{\mu^g}\left[-grad p^g+\rho^g\mathbf{g}\right]\right)-\beta_s\left[1-n\right]S_g\dot{T}=0$$ gaMBE

4) $$\left[C_p^w nS_w\rho^w\frac{k^{rw}\mathbf{k}_w}{\mu^w}\left[-grad\left(p^g-p^c\right)+\rho^w\mathbf{g}\right]+C_p^g nS_g\rho^g\frac{k^{rg}\mathbf{k}_g}{\mu^g}\left[-grad p^g+\rho^g\mathbf{g}\right]\right]\cdot grad T+\left(\rho C_p\right)_{eff}\dot{T}-$$
$$div\left(\chi_{eff}\, grad T\right)-\rho^w\frac{nS_w}{K_w}\Delta H_{vap}\left[\dot{p}^g-\dot{p}^c\right]-\Delta H_{vap}\rho^w S_w\alpha\,\mathbf{mL\dot{u}}+\Delta H_{vap}\beta_{sw}\dot{T}-n\Delta H_{vap}\dot{S}_w\left[\rho^w-\rho^{gw}\right]-$$
$$div\left(\rho^w\frac{k^{rw}\mathbf{k}_w}{\mu^w}\left[-grad\left(p^g-p^c\right)+\rho^w\mathbf{g}\right]\right)\Delta H_{vap}=\boldsymbol{\sigma}'\dot{\boldsymbol{\varepsilon}}^p$$ EBE

State variables: $\mathbf{u}$ p^g p^c T

Initial and boundary conditions

Initial conditions

$$p^g = p^g_0\,, \quad p^c = p^c_0\,, \quad T = T_0\,, \quad \mathbf{u} = \mathbf{u}_0\,, \quad \dot{\mathbf{u}} = \dot{\mathbf{u}}_0\,, \quad \text{at} \quad t = t_0$$

Boundary conditions

$$\begin{array}{lllll} p^g = \hat{p}^g & \text{on} & \partial B_g\,, & p^c = \hat{p}^c & \text{on} \quad \partial B_c\,, \\ T = \hat{T} & \text{on} & \partial B_T\,, & \mathbf{u} = \hat{\mathbf{u}} & \text{on} \quad \partial B_u \quad \text{for} \quad t \geq t_0 \end{array}$$

$$\begin{aligned} [nS_g\rho^{ga}\,\mathbf{v}^{gs}]\cdot\mathbf{n} &= q^{ga} \qquad \text{on } \partial B^q_g, \\ [nS_g\rho^{gw}\,\mathbf{v}^{gs} + nS_w\rho^w\,\mathbf{v}^{ws}]\cdot\mathbf{n} &= \beta_c\left(\rho^{gw} - \rho^{gw}_\infty\right) \\ &\quad + q^{gw} + q^w \text{ on } \partial B^q_c \\ [nS_w\rho^w\,\mathbf{v}^{ws}\,\Delta H_{vap} - \chi_{eff}\,grad(T)\,]\cdot\mathbf{n} &= \alpha_c\,(T - T_\infty) \\ &\quad + e\sigma_0(T^4 - T^4_\infty) + q^T \quad \text{on } \partial B^q_T \\ \boldsymbol{\sigma}\cdot\mathbf{n} &= \mathbf{t} \quad \text{on} \quad \partial B^q_u \end{aligned}$$

Non-isothermal constitutive models: fluids

(*Gawin and Schrefler EC96; Lewis and Schrefler 98*)

gas phase = mixture of dry air and water vapour (perfect gases)

Clapeyron's equation and Dalton's law

$$p^{ga} = \rho^{ga} RT/M_a \qquad p^{gw} = \rho^{gw} RT/M_w$$

$$p^g = p^{ga} + p^{gw} \qquad \rho^g = \rho^{ga} + \rho^{gw}$$

Kelvin-Laplace's equation $$p^{gw} = p^{gws}(T)\ \exp\left(-\frac{p^c M_w}{\rho^w RT}\right)$$

Clausius-Clapeyron's equation $$p^{gws}(T) = p^{gwso}\ \exp\left(-\frac{M_w \Delta H_{gw}}{R}\left(\frac{1}{T} - \frac{1}{T_0}\right)\right)$$

Non-isothermal constitutive models: fluids

(*Gawin, Schrefler EC96; Lewis, Schrefler 98*)

Darcy, Fick: from linearization of 2nd principle of thermodynamics

Fick law
$$\mathbf{v}_g^{ga} = -\frac{M_a M_w}{M_g^2}\mathbf{D}_g \,\mathrm{grad}\left(\frac{p^{ga}}{p^g}\right) = -\mathbf{v}_g^{gw}$$

Darcy law
$$nS_\pi \mathbf{v}^{\pi s} = \frac{k^{r\pi}\mathbf{k}_\pi}{\mu^\pi}\left[-grad\left(p^\pi\right)+\rho^\pi \mathbf{g}\right]$$

Fourier law
$$\boldsymbol{q} = -\chi_{eff}\, grad\,(T)$$

Dynamic viscosity of gas
$$\mu^g = \mu^{gw} + [\mu^{ga} - \mu^{gw}]\left(\frac{p^{ga}}{p^g}\right)^{0.608}$$
$$\mu^{gw} = \mu^{gw0} + \alpha^{gw}(T - T_0)$$
$$\mu^{ga} = \mu^{ga0} + \alpha^{ga}(T - T_0) + \beta^{ga}(T - T_0)^2$$

Non-isothermal constitutive models: fluids

(*Gawin, Majorana, Schrefler MCFM 1999;*
Gawin, Pesavento, Schrefler NAG 2002;
Gawin, Pesavento FT 2011
for concrete as multiphase porous material)

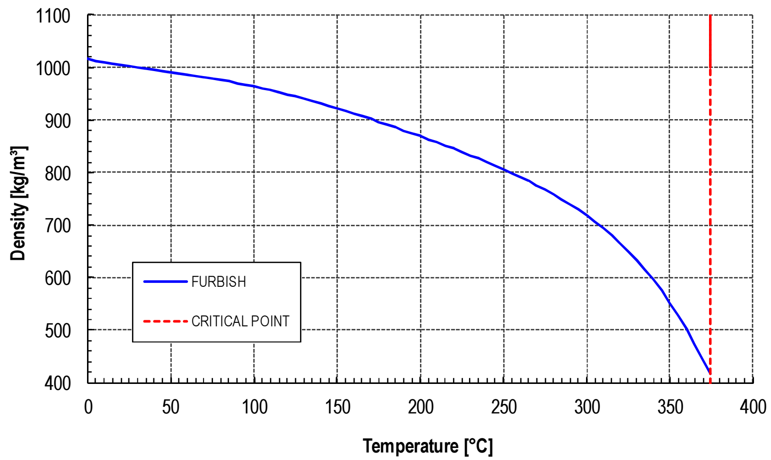

Bulk density of liquid water *(Furbish, 1997)*

$$\rho^w = [b_0 + b_1(T) + b_2(T)^2 + b_3(T)^3 + b_4(T)^4 + b_5(T)^5]$$
$$+K[a_0 + a_1(T) + a_2(T)^2 + a_3(T)^3 + a_4(T)^4 + a_5(T)^5]$$

Dynamic viscosity of liquid water $\mu^w = 0.6612\text{x}[T - 229]^{1.562}$

Enthalpy of evaporation *(Watson formula)*

$$\Delta H_{vap} = 2.672\text{E}{+}5\text{x}[T_{cr} - T]^{0.38} \quad \text{with} \quad T_{cr} = 647.3\text{K}$$

Constitutive models: hydraulic behaviour

$S_w(p^c, T, \varepsilon_v^p)$, $k^{rw}(p^c, \cancel{T})$, $k^{rg}(p^c, \cancel{T})$: experimental functions

(Monfared et al. EG 2012)

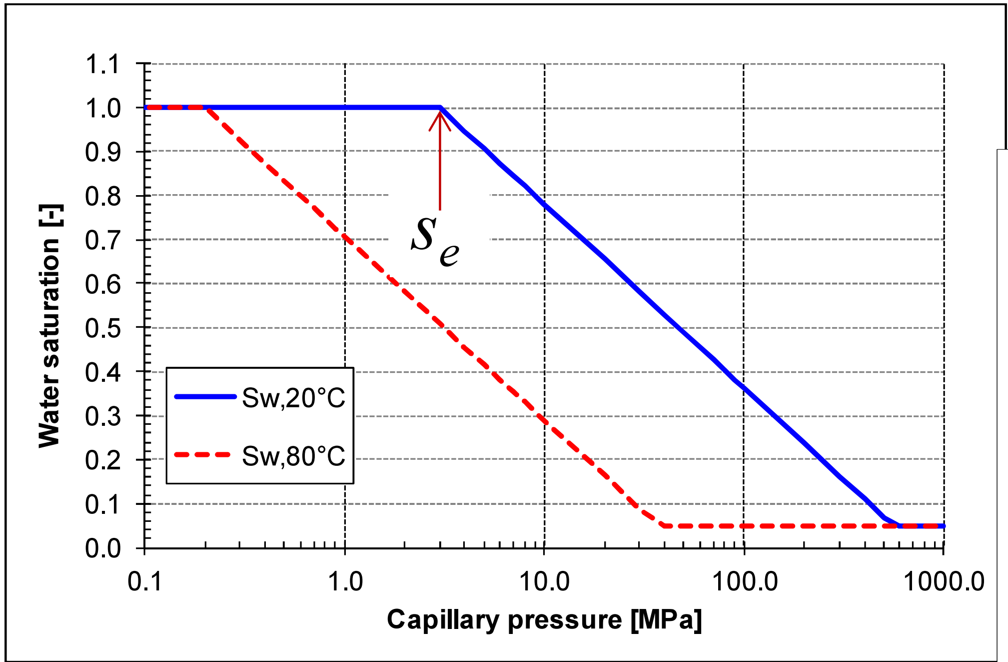

$S_w - p^c$

(François and Laloui, NAG08)

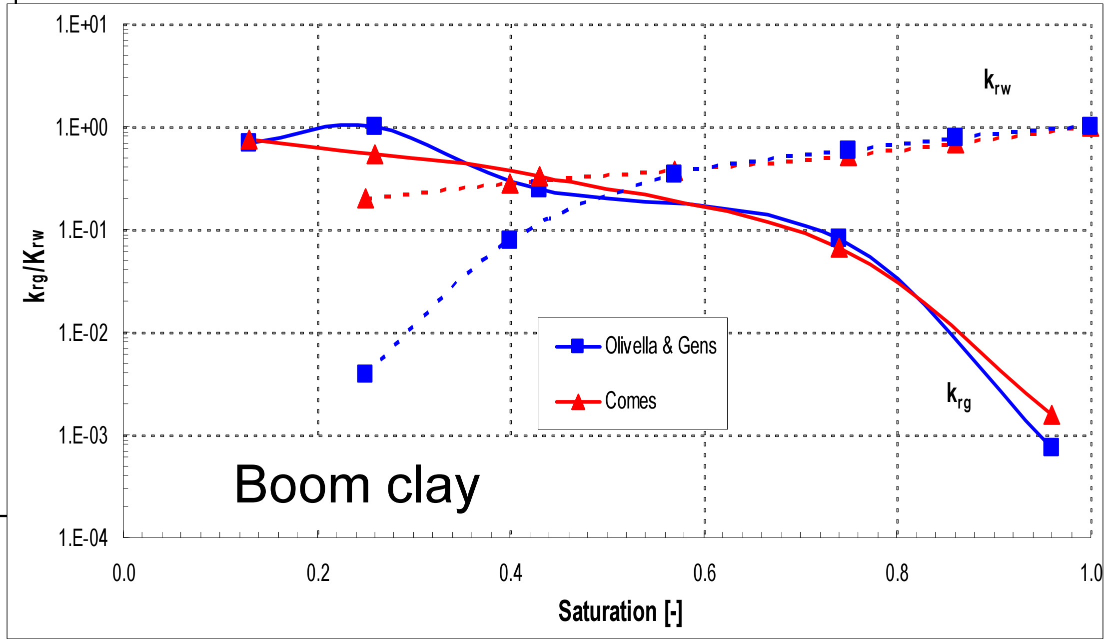

k^{rw} - S_w and $k^{rg} - S_w$

(Olivella and Gens, TIPM 2000)

Air entry value:

$$s_e = s_{e0} \cdot e^{-\beta_H \cdot \Delta S_r} \left[1 - \theta_T \log \frac{T}{T_0} - \theta_e \log(1 - \varepsilon_v^p) \right]$$

Constitutive models: solid skeleton

(isothermal/non-isothermal & variably saturated conditions)

Classical rate-independent elasto-plasticity

Drucker-Prager (non associated plastic flow,

linear isotropic hardening)

(implicit) return mapping algorithm

(Sanavia, Steinmann, Schrefler, CM 2002)

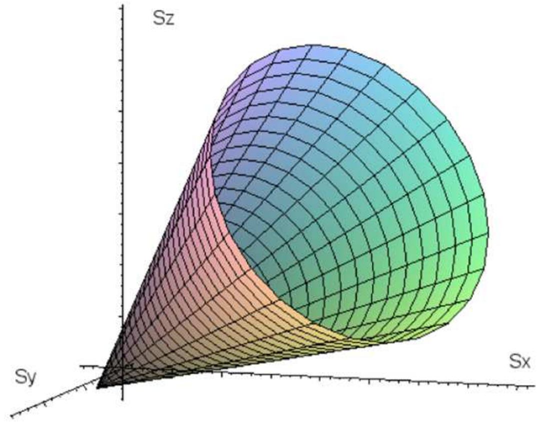

with suction dependent cohesion:

$c = c_0 + p^c \tan \varphi'_b$ (*Fredlund et al. 1978*)

$c = c_0 + p^c \tan \varphi'_b - T \tan \varphi'_t$ (*non-isothermal cond.*)

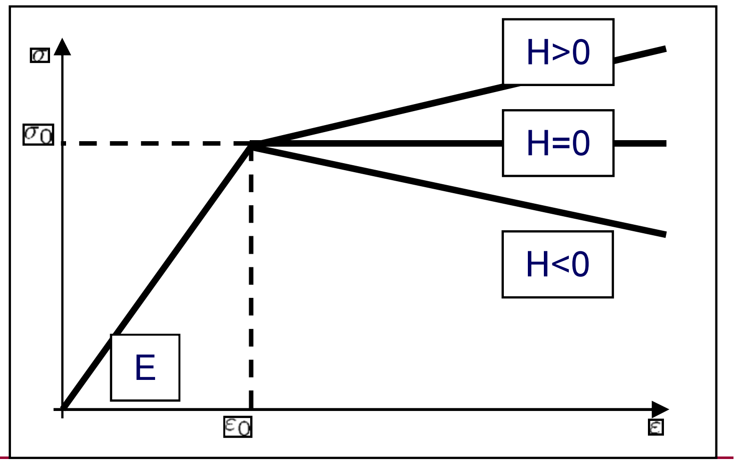

Non-isothermal constitutive models: solid skeleton

ACMEG-TS model (Advanced Constitutive Model for Environmental Geomechanics -*Thermal* and *Suction* effects) for clayey soils

(Laloui, François NAG08; Laloui, François JEM09, …)

Critical state concept, multi-surface plasticity *(ECP-Hujeux model)*

and bounding surface theory

$$\dot{\varepsilon}_{ij} = \dot{\varepsilon}_{ij}^{Te} + \dot{\varepsilon}_{ij}^{Tp}$$

$$\dot{\varepsilon}_{ij}^{Te} = \dot{\varepsilon}_{ij}^{me} + \frac{\beta'_s}{3}\dot{T}\,\mathrm{I}_{ij}$$

Non-linear thermal elasticity

(thermo hypo-elasticity)

$$\begin{cases} K = K_{ref}\left(\dfrac{p'}{p_{ref}}\right)^n \qquad G = G_{ref}\left(\dfrac{p'}{p_{ref}}\right)^n \\ \beta'_s = \left(\beta'_{s0} + \zeta \cdot T\right)\left(\dfrac{p'_{c0}}{p'}\right)^n \end{cases}$$

Non-isothermal constitutive models: solid skeleton

Thermo-plasticity $$\dot{\varepsilon}_{ij}^{Tp} = \sum_{k=1}^{2} \dot{\varepsilon}_{ij,k}^{Tp} = \dot{\varepsilon}_{ij,\mathrm{ISO}}^{Tp} + \dot{\varepsilon}_{ij,\mathrm{DEV}}^{Tp} = \sum_{k=1}^{2} \dot{\lambda}_k \frac{\partial Q_k}{\partial \sigma'_{ij}}$$

linear combination of two irreversible contributions

(developed within the multi-mechanism plasticity theory, *Koiter 1960*)

$$f_{iso} = p' - p'_{c0}(T_0) e^{\varepsilon_v^p} \left[1 - \gamma_T \log(T/T_0)\right]\left[1 + \gamma_s \log(s/s_e)\right] r_{iso} = 0$$

Isotropic thermo-plastic yield function

Deviatoric thermo-plastic yield function

$$f_{dev} = q - Mp' \left(1 - b \ln \frac{d \cdot p'}{p'_{c0}(T_0) \cdot e^{\varepsilon_v^p} \cdot \left[1 - \gamma_T \log(T/T_0)\right]\left[1 + \gamma_s \log(s/s_e)\right]} \right) r_{dev} = 0$$

$$M(T) = M_0 - g(T - T_0)$$

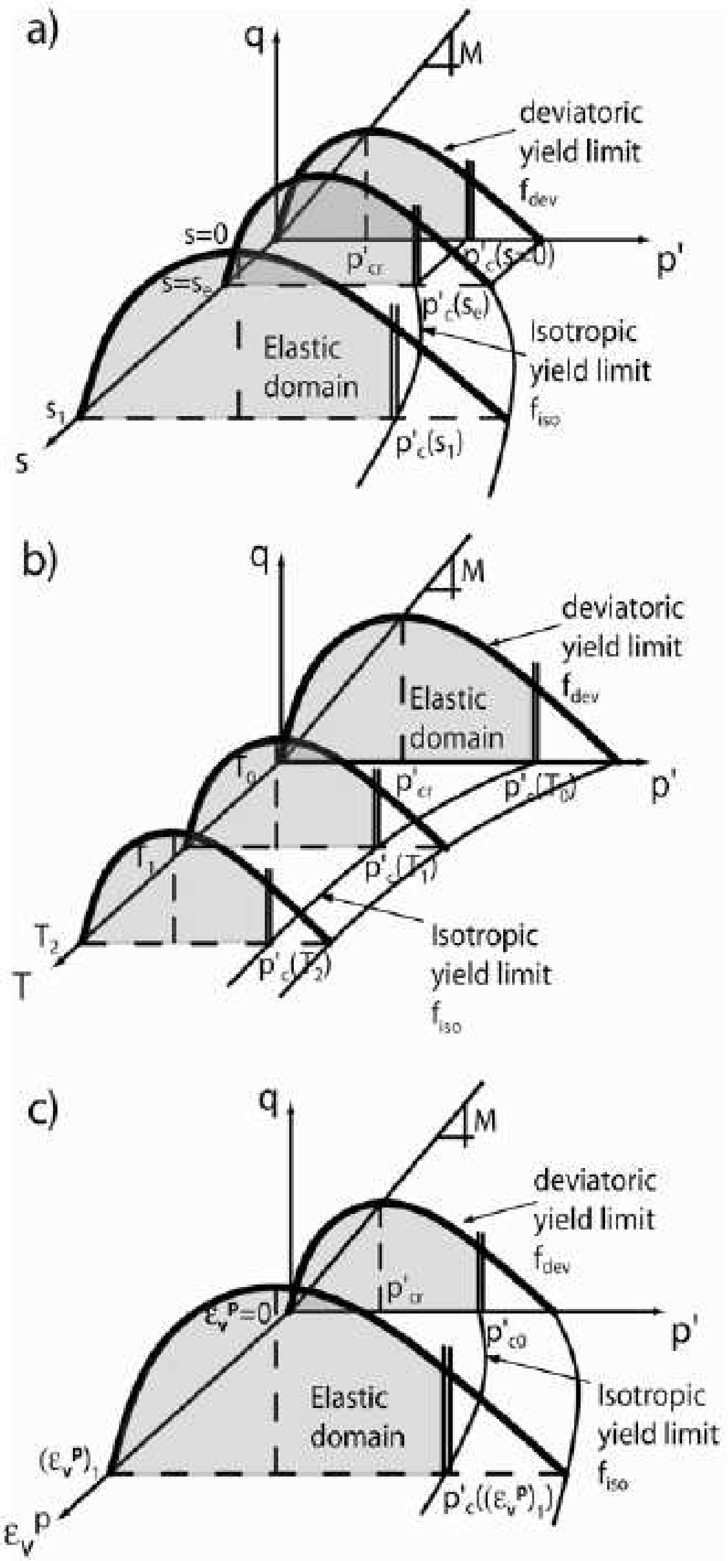

nstitutive models: solid skeleton

$$= \sum_{k=1}^{2} \dot{\varepsilon}^{Tp}_{ij,k} = \dot{\varepsilon}^{Tp}_{ij,\mathrm{ISO}} + \dot{\varepsilon}^{Tp}_{ij,\mathrm{DEV}} = \sum_{k=1}^{2} \dot{\lambda}_k \frac{\partial Q_k}{\partial \sigma'_{ij}}$$

irreversible contributions (multi-mechanism

er 1960)

$$_T \log\left(T/T_0\right)\right]\left[1+\gamma_s \log\left(s/s_e\right)\right] r_{iso} = 0$$

ld function

eld function

$$\frac{d \cdot p'}{T_0)\cdot e^{\varepsilon_v^p}\cdot\left[1-\gamma_T \log\left(T/T_0\right)\right]\left[1+\gamma_s \log\left(s/s_e\right)\right]}\Bigg) r_{dev} = 0$$

Finite Element discretisation

Mathematical model: non-linear coupled PDEs

↓

Non-linear system of algebraic equations

- Incremental approach
- Spatial discretisation: standard Galerkin method, isoparametric formulation
- Time discretisation: Generalized Newmark method (GN22)

Summary of the F.E. approximation

1) $\mathbf{A}(\phi) = \mathbf{0}$ in Ω (domain)

$\mathbf{B}(\phi) = \mathbf{0}$ on Γ (boundary)

} strong form

non-linear system of partial differential equations

2) Weigthed residual method ⟹ weak (integral) form of $\left\{ \begin{array}{l} \mathbf{A}(\phi) = \mathbf{0} \\ \mathbf{B}(\phi) = \mathbf{0} \end{array} \right.$

3) Discretisation in space

4) Discretisation in time

} non-linear system of algebric equations

5) (consistent) linearisation ⟹ linearised system of algebric equations which can be solved numerically

(Newton-Rapson procedure)

(Textbooks: *Zienkiewicz O.C. and R. Taylor, T.J. Hughes, ... P. Wriggers*)

Weak formulation: weigthed residual method

Standard approach

Test functions: $\delta \mathbf{u}_s$ (virtual displacements); δp^g (virtual gas pressure)

δp^c (virtual capillary pressure); δT (virtual temperature)

LMBE:

$$\int_B \left(div\,\boldsymbol{\sigma} + \rho\left[\mathbf{g} - \mathbf{a}\right]\right) \cdot \delta \mathbf{u}_s \, d\,\mathrm{v} = 0 \qquad \forall \delta \mathbf{u}_s \neq \mathbf{0}$$

Green's theorem

$$-\int_B \boldsymbol{\sigma}' : grad\,\delta \mathbf{u}_s \, d\,\mathrm{v} \quad + \int_B \left(p^g - S_w p^c \right) \mathrm{div}\delta \mathbf{u}_s \, d\,\mathrm{v}$$

$$+ \int_B \rho\left[\mathbf{g} - \mathbf{a}\right] \cdot \delta \mathbf{u}_s \, d\,\mathrm{v} + \int_{\partial B} \bar{\mathbf{t}} \cdot \delta \mathbf{u}_s \, da = 0 \quad \forall \delta \mathbf{u}_s \neq \mathbf{0}$$

…similarly for the other governing equations

Discretization in space:

- Note that the choice of the shape functions must be of C_0 continuity.

- Among various possible element combinations, the mixed elements are recommended to satisfy the LBB conditions or to pass the patch test (e.g. for 2D problems) - (*Zienkiewicz et al. 1999*):

(1) 6-noded quadratic triangle for the displacements and 3-noded linear triangle for the water pressure.

(2) 9-noded (or 8) biquadratic quadrilateral for the displacements and 4-noded bilinear quadrilateral for the water pressure.

Mixed finite elements (in 2D)

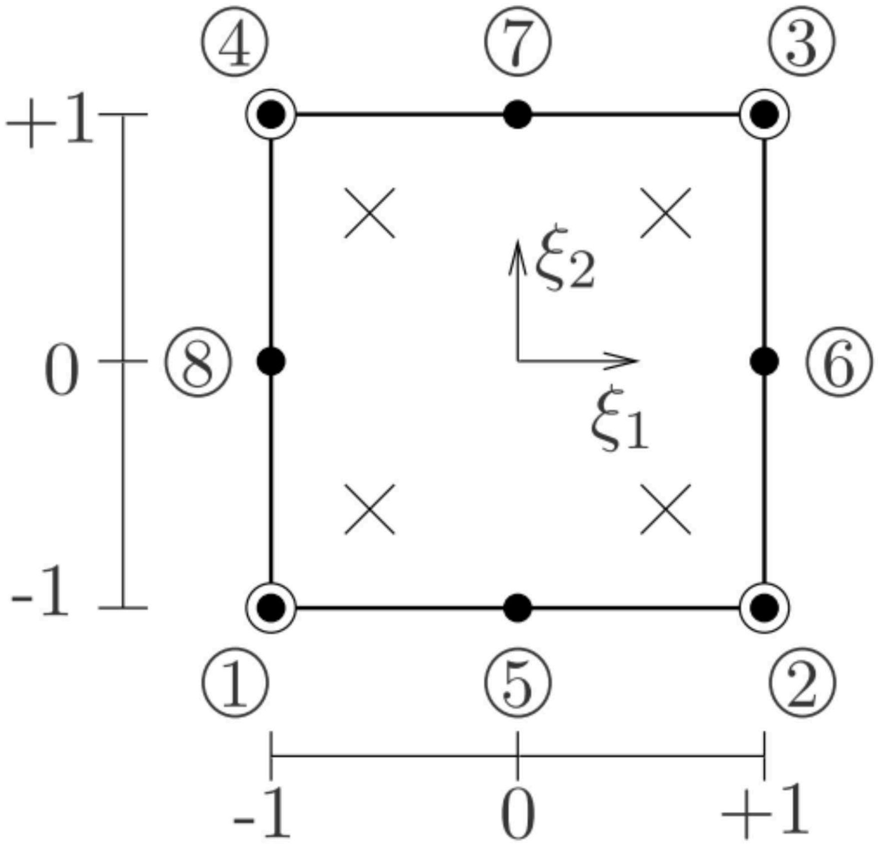

- ● Solid skeleton displacement
- ○ Fluid pressure/temperature

$$\begin{cases} p^g = \mathbf{N}_g \bar{\mathbf{p}}^g & \text{Gas pressure} \\ p^c = \mathbf{N}_c \bar{\mathbf{p}}^c & \text{Capillary pressure} \\ T = \mathbf{N}_T \bar{\mathbf{T}} & \text{Temperature} \\ \mathbf{u} = \mathbf{N}_u \bar{\mathbf{u}} & \text{Displacement} \end{cases}$$

$\mathbf{N}_u$: Bi-quadratic functions

$\mathbf{N}_g, \mathbf{N}_c, \mathbf{N}_T$: Bi-linear functions

Discretization in space:

$$
\begin{cases}
\boldsymbol{C}_{gg}\dot{\overline{p}}^{g} + \boldsymbol{C}_{gc}\dot{\overline{p}}^{c} - \boldsymbol{C}_{gT}\dot{\overline{T}} + \boldsymbol{C}_{gu}\dot{\overline{u}} + \boldsymbol{K}_{gg}\overline{p}^{g} - \boldsymbol{K}_{gc}\overline{p}^{c} - \boldsymbol{K}_{gT}\overline{T} = \boldsymbol{f}_{g} \\
\boldsymbol{C}_{cg}\dot{\overline{p}}^{g} + \boldsymbol{C}_{cc}\dot{\overline{p}}^{c} + \boldsymbol{C}_{cT}\dot{\overline{T}} + \boldsymbol{C}_{cu}\dot{\boldsymbol{u}} + \boldsymbol{K}_{cg}\overline{p}^{g} + \boldsymbol{K}_{cc}\overline{p}^{c} + \boldsymbol{K}_{cT}\overline{T} = \boldsymbol{f}_{c} \\
-\boldsymbol{C}_{Tg}\dot{\overline{p}}^{g} - \boldsymbol{C}_{Tc}\dot{\overline{p}}^{c} + \boldsymbol{C}_{TT}\dot{\overline{T}} - \boldsymbol{C}_{Tu}\dot{\overline{u}} - \boldsymbol{K}_{Tg}\overline{p}^{g} + \boldsymbol{K}_{Tc}\overline{p}^{c} + \boldsymbol{K}_{TT}\overline{T} = \boldsymbol{f}_{T} \\
\boldsymbol{M}_{uu}\ddot{\overline{\boldsymbol{u}}} + \int \boldsymbol{B}^{T}\boldsymbol{\sigma}' dV - \boldsymbol{K}_{ug}\overline{p}^{g} + \boldsymbol{K}_{uc}\overline{p}^{c} = \boldsymbol{f}_{u}
\end{cases}
$$

Parabolic equations

Hyperbolic equations

System of partial differential equations

- 1° and 2° order

- Fully coupled

Discretization in time: Generalized Newmark Method (GN22)

(Zienkiewicz, Taylor, 2002)

$$\dot{\mathbf{u}}^{n+1} = \dot{\mathbf{u}}^{n} + \Delta t \ddot{\mathbf{u}}^{n} + \beta_1 \Delta t \Delta \ddot{\mathbf{u}}^{n}$$

$$\mathbf{u}^{n+1} = \mathbf{u}^{n} + \Delta t \dot{\mathbf{u}}^{n} + \frac{1}{2}\Delta t^2 \ddot{\mathbf{u}}^{n} + \frac{1}{2}\beta_2 \Delta t^2 \Delta \ddot{\mathbf{u}}^{n}$$

$$\overline{T}^{n+1} = \overline{T}^{n} + \Delta t \dot{\overline{T}}^{n} + \alpha \Delta t \Delta \dot{\overline{T}}^{n}$$

$$\overline{p}^{c\,n+1} = \overline{p}^{c\,n} + \Delta t \dot{\overline{p}}^{c\,n} + \vartheta \Delta t \Delta \dot{\overline{p}}^{c\,n}$$

$$\overline{p}^{g\,n+1} = \overline{p}^{g\,n} + \Delta t \dot{\overline{p}}^{g\,n} + \theta \Delta t \Delta \dot{\overline{p}}^{g\,n}$$

$$\Delta \ddot{\mathbf{u}}^{n} = \ddot{\mathbf{u}}^{n+1} - \ddot{\mathbf{u}}^{n}$$

$$\Delta \dot{\overline{T}}^{n} = \dot{\overline{T}}^{n+1} - \dot{\overline{T}}^{n}$$

$$\Delta \dot{\overline{p}}^{c\,n} = \dot{\overline{p}}^{c\,n+1} - \dot{\overline{p}}^{c\,n}$$

$$\Delta \dot{\overline{p}}^{g\,n} = \dot{\overline{p}}^{g\,n+1} - \dot{\overline{p}}^{g\,n}$$

$$\boxed{\frac{1}{2} \le \beta_1, \alpha, \vartheta, \theta \le 1 \qquad \frac{1}{2} \le \beta_1 \le \beta_2}$$

Unconditionally stability condition

Finite Element discretisation

Mathematical model: non-linear coupled PDEs

Non-linear system of algebraic equations

Linearisation (directional derivatives)

$$\left.\frac{\partial \psi^k}{\partial \boldsymbol{X}}\right|_{\boldsymbol{X}^i_{n+1}} \Delta \boldsymbol{X}^{i+1}_{n+1} = -\psi^k(\boldsymbol{X}^i_{n+1})$$

Solution of the final set of linearized equations (monolithic approach)

- Incremental approach
- Spatial discretisation: standard Galerkin method, isoparametric formulation
- Time discretisation: Generalized Newmark method (GN22)

Numerical validation (Comes-Geo fem code – Unipd, I)

http://www.dicea.unipd.it/

1. Validation of the **isothermal solid phase model** 1 eq.

    1a- Wave propagation problem in a solid bar - (analytical solution)

    1b- Wave propagation problem in a dry sand column (numerical comparison)

2. Validation of the **isothermal water saturated model** 2 eqs.

    Dynamic consolidation - (analytical solution)

3. Validation of the **non-isothermal water saturated model** 3 eqs.

    Non-isothermal consolidation - (Aboustit et al. numerical test)

4. Validation of the **isothermal variably saturated model** 3 eqs.

    4a- Liakopoulos test: quasi-static drainage of liquid water from an initially water saturated sand column - (numerical benchmark)

    4b- Unsaturated sand column subjected to a step load (numerical comparison)

Numerical validation (Comes-Geo fem code – Unipd, I)

http://www.dicea.unipd.it/

1. Validation of the **isothermal solid phase model**

   1a- Wave propagation problem in a solid bar - (analytical solution)

   1b- Wave propagation problem in a dry sand column (numerical comparison)

2. Validation of the **isothermal water saturated model**

   Dynamic consolidation - (analytical solution)

3. Validation of the **non-isothermal water saturated model**

   Non-isothermal consolidation - (Aboustit et al. numerical test)

4. Validation of the **isothermal variably saturated model**

   4a- Liakopoulos test: quasi-static drainage of liquid water from an initially water saturated sand column - (numerical benchmark)

   4b- Unsaturated sand column subjected to a step load (numerical comparison)

Numerical validation (Comes-Geo fem code – Unipd, I)

1) $$div\left(\boldsymbol{\sigma}' - \left[p^g - S_w p^c\right]\mathbf{I}\right) + \rho\mathbf{g} - \rho\mathbf{a}^s = \mathbf{0} \longrightarrow div\left(\boldsymbol{\sigma}\right) + \rho\mathbf{g} - \rho\mathbf{a}^s = \mathbf{0}$$ LMBE

2) $$\rho^w \frac{nS_w}{K_w}\left[\dot{p}^g - \dot{p}^c\right] + \left[\rho^w S_w + \rho^{gw} S_g\right]\alpha div\mathbf{v}^s - \left[\rho^w \beta_{sw} + \rho^{gw}\beta_s[1-n]S_g\right]\dot{T} + nS_g\dot{\rho}^{gw}$$
$$+ div\mathbf{J}_g^{gw} + n\left[\rho^w - \rho^{gw}\right]\dot{S}_w + div\left(\rho^w \frac{k^{rw}\mathbf{k}_w}{\mu^w}\left[-grad\left(p^g - p^c\right) + \rho^w\mathbf{g}\right]\right) +$$
$$+ div\left(\rho^{gw}\frac{k^{rgw}\mathbf{k}_g}{\mu^{gw}}\left[-gradp^{gw} + \rho^{gw}\mathbf{g}\right]\right) = 0$$ wsMBE

3) $$\alpha S_g div\mathbf{v}^s + \frac{nS_g}{\rho^{ga}}\dot{\rho}^{ga} + \frac{1}{\rho^{ga}}div\mathbf{J}_g^{ga} - n\dot{S}_w +$$
$$+ \frac{1}{\rho^{ga}}div\left(\rho^{ga}\frac{k^{rg}\mathbf{k}_g}{\mu^g}\left[-gradp^g + \rho^g\mathbf{g}\right]\right) - \beta_s[1-n]S_g\dot{T} = 0$$ gaMBE

4) $$\left[C_p^w nS_w\rho^w \frac{k^{rw}\mathbf{k}_w}{\mu^w}\left[-grad\left(p^g - p^c\right) + \rho^w\mathbf{g}\right] + C_p^g nS_g\rho^g \frac{k^{rg}\mathbf{k}_g}{\mu^g}\left[-gradp^g + \rho^g\mathbf{g}\right]\right]\cdot grad\,T + \left(\rho C_p\right)_{eff}\dot{T} -$$
$$div\left(\chi_{eff}\,grad\,T\right) - \rho^w \frac{nS_w}{K_w}\Delta H_{vap}\left[\dot{p}^g - \dot{p}^c\right] - \Delta H_{vap}\rho^w S_w \alpha\,\mathbf{mL\dot{u}} + \Delta H_{vap}\beta_{sw}\dot{T} - n\Delta H_{vap}\dot{S}_w\left[\rho^w - \rho^{gw}\right] -$$
$$div\left(\rho^w \frac{k^{rw}\mathbf{k}_w}{\mu^w}\left[-gradp^w + \rho^w\mathbf{g}\right]\right)\Delta H_{vap} = \boldsymbol{\sigma}'\dot{\boldsymbol{\varepsilon}}^p$$ EBE

Numerical validation (Comes-Geo fem code – Unipd, I)

http://www.dicea.unipd.it/

1. Validation of the **isothermal solid phase model**

   1a- Wave propagation problem in a solid bar - (analytical solution)

   1b- Wave propagation problem in a dry sand column (numerical comparison)

2. Validation of the **isothermal water saturated model**

   Dynamic consolidation - (analytical solution)

3. Validation of the **non-isothermal water saturated model**

   Non-isothermal consolidation - (Aboustit et al. numerical test)

4. Validation of the **isothermal variably saturated model**

   4a- Liakopoulos test: quasi-static drainage of liquid water from an initially water saturated sand column - (numerical benchmark)

   4b- Unsaturated sand column subjected to a step load (numerical comparison)

Numerical validation (Comes-Geo fem code – Unipd, I)

1) $$div\left(\boldsymbol{\sigma}'-\left[p^g - S_w p^c\right]\mathbf{I}\right)+\rho\mathbf{g}-\rho\mathbf{a}^s=\mathbf{0} \quad \text{with} \quad S_w=1 \quad p^g - p^c = p^w$$

LMBE

2) $$\rho^w \frac{nS_w}{K_w}\left[\dot p^g-\dot p^c\right]+\left[\rho^w S_w+\cancel{\rho^{gw}}S_g\right]\alpha div\mathbf{v}^s \cancel{-\left[\rho^w\beta_{sw}+\rho^{gw}\beta_s[1-n]S_g\right]\dot T} + \cancel{nS_g\dot\rho^{gw}}$$

$$\cancel{+div\mathbf{J}_g^{gw}} + n\left[\rho^w-\cancel{\rho^{gw}}\right]\dot S_w + div\left(\rho^w\frac{k^{rw}\mathbf{k}_w}{\mu^w}\left[-grad\left(p^g-p^c\right)+\rho^w\mathbf{g}\right]\right)+$$

$$\cancel{+div\left(\rho^{gw}\frac{k^{rgw}\mathbf{k}_g}{\mu^{gw}}\left[-gradp^{gw}+\rho^{gw}\mathbf{g}\right]\right)}=0$$

wsMBE

3) $$\alpha S_g div\mathbf{v}^s+\frac{nS_g}{\rho^{ga}}\dot\rho^{ga}+\frac{1}{\rho^{ga}}div\mathbf{J}_g^{ga}-n\dot S_w+$$

$$+\frac{1}{\rho^{ga}}div\left(\rho^{ga}\frac{k^{rg}\mathbf{k}_g}{\mu^g}\left[-gradp^g+\rho^g\mathbf{g}\right]\right)-\beta_s[1-n]S_g\dot T=0$$

gaMBE

4) $$\left[C_p^w nS_w\rho^w\frac{k^{rw}\mathbf{k}_w}{\mu^w}\left[-grad\left(p^g-p^c\right)+\rho^w\mathbf{g}\right]+C_p^g nS_g\rho^g\frac{k^{rg}\mathbf{k}_g}{\mu^g}\left[-gradp^g+\rho^g\mathbf{g}\right]\right]\cdot grad\,T+\left(\rho C_p\right)_{eff}\dot T-$$

$$div\left(\chi_{eff}\,grad\,T\right)-\rho^w\frac{nS_w}{K_w}\Delta H_{vap}\left[\dot p^g-\dot p^c\right]-\Delta H_{vap}\rho^w S_w\alpha\,\mathbf{mL\dot u}+\Delta H_{vap}\beta_{sw}\dot T-n\Delta H_{vap}\dot S_w\left[\rho^w-\rho^{gw}\right]-$$

$$div\left(\rho^w\frac{k^{rw}\mathbf{k}_w}{\mu^w}\left[-gradp^w+\rho^w\mathbf{g}\right]\right)\Delta H_{vap}=\boldsymbol{\sigma}'\dot{\boldsymbol{\varepsilon}}^p$$

EBE

Numerical validation (Comes-Geo fem code – Unipd, I)

http://www.dicea.unipd.it/

1. Validation of the **isothermal solid phase model**

   1a- Wave propagation problem in a solid bar - (analytical solution)

   1b- Wave propagation problem in a dry sand column (numerical comparison)

2. Validation of the **isothermal water saturated model**

   Dynamic consolidation - (analytical solution)

3. Validation of the **non-isothermal water saturated model**

   Non-isothermal consolidation - (Aboustit et al. <u>numerical test</u>)

4. Validation of the **isothermal variably saturated model**

   4a- Liakopoulos test: quasi-static drainage of liquid water from an initially water saturated sand column - (numerical benchmark)

   4b- Unsaturated sand column subjected to a step load (numerical comparison)

Numerical validation (Comes-Geo fem code – Unipd, I)

1) $$div\left(\boldsymbol{\sigma}'-\left[p^g - S_w p^c\right]\mathbf{I}\right)+\rho\mathbf{g}-\rho\mathbf{a}^s=\mathbf{0} \quad \text{with} \quad S_w = 1 \quad p^g - p^c = p^w$$ LMBE

2) $$\rho^w \frac{nS_w}{K_w}\left[\dot{p}^g-\dot{p}^c\right]+\left[\rho^w S_w+\cancel{\rho^{gw} S_g}\right]\alpha div\mathbf{v}^s-\left[\rho^w\beta_{sw}+\rho^{gw}\beta_s[1-n]S_g\right]\dot{T}+\cancel{nS_g\dot{\rho}^{gw}}$$

wsMBE

$$+\cancel{div\mathbf{J}_g^{gw}}+n\left[\rho^w-\rho^{gw}\right]\dot{S}_w+div\left(\rho^w\frac{k^{rw}\mathbf{k}_w}{\mu^w}\left[-grad\left(p^g-p^c\right)+\rho^w\mathbf{g}\right]\right)+$$

$$\cancel{+div\left(\rho^{gw}\frac{k^{rgw}\mathbf{k}_g}{\mu^{gw}}\left[-gradp^{gw}+\rho^{gw}\mathbf{g}\right]\right)}=0$$

3) $$\cancel{\alpha S_g div\mathbf{v}^s+\frac{nS_g}{\rho^{ga}}\dot{\rho}^{ga}+\frac{1}{\rho^{ga}}div\mathbf{J}_g^{ga}-n\dot{S}_w+\frac{1}{\rho^{ga}}div\left(\rho^{ga}\frac{k^{rg}\mathbf{k}_g}{\mu^g}\left[-gradp^g+\rho^g\mathbf{g}\right]\right)-\beta_s[1-n]S_g\dot{T}=0}$$ gaMBE

4) $$\left[C_p^w nS_w\rho^w\frac{k^{rw}\mathbf{k}_w}{\mu^w}\left[-grad\left(p^g-p^c\right)+\rho^w\mathbf{g}\right]+\cancel{C_p^g nS_g\rho^g\frac{k^{rg}\mathbf{k}_g}{\mu^g}\left[-gradp^g+\rho^g\mathbf{g}\right]}\right]\cdot grad\,T+\left(\rho C_p\right)_{eff}\dot{T}-$$

$$div\left(\chi_{eff}\,grad\,T\right)-\cancel{\rho^w\frac{nS_w}{K_w}\Delta H_{vap}\left[\dot{p}^g-\dot{p}^c\right]}-\cancel{\Delta H_{vap}\rho^w S_w\alpha\,\mathbf{mL\dot{u}}}+\Delta H_{vap}\beta_{sw}\dot{T}-\cancel{n\Delta H_{vap}\dot{S}_w\left[\rho^w-\rho^{gw}\right]}-$$

$$div\left(\rho^w\frac{k^{rw}\mathbf{k}_w}{\mu^w}\left[-gradp^w+\rho^w\mathbf{g}\right]\right)\Delta H_{vap}=\boldsymbol{\sigma}'\dot{\boldsymbol{\varepsilon}}^p$$ EBE

Numerical validation (Comes-Geo fem code – Unipd, I)

http://www.dicea.unipd.it/

1. Validation of the **isothermal solid phase model**

   1a- Wave propagation problem in a solid bar - (analytical solution)

   1b- Wave propagation problem in a dry sand column (numerical comparison)

2. Validation of the **isothermal water saturated model**

   Dynamic consolidation - (analytical solution)

3. Validation of the **non-isothermal water saturated model**

   Non-isothermal consolidation - (Aboustit et al. numerical test)

4. Validation of the **isothermal variably saturated model**

   4a- Liakopoulos test: quasi-static drainage of liquid water from an initially water saturated sand column - (numerical benchmark)

   4b- Unsaturated sand column subjected to a step load (numerical comparison)

Numerical validation (Comes-Geo fem code – Unipd, I)

1) $$div\left(\boldsymbol{\sigma}' - \left[p^g - S_w p^c\right]\mathbf{I}\right) + \rho\mathbf{g} - \rho\mathbf{a}^s = \mathbf{0} \quad \text{with} \quad S_w = 1 \quad p^g - p^c = p^w$$

LMBE

2) $$\rho^w \frac{nS_w}{K_w}\left[\dot{p}^g - \dot{p}^c\right] + \left[\rho^w S_w + \rho^{gw} S_g\right]\alpha div\mathbf{v}^s - \left[\rho^w \beta_{sw} + \rho^{gw}\beta_s[1-n]S_g\right]\dot{T} + nS_g\dot{\rho}^{gw}$$

$$+ div\mathbf{J}_g^{gw} + n\left[\rho^w - \rho^{gw}\right]\dot{S}_w + div\left(\rho^w \frac{k^{rw}\mathbf{k}_w}{\mu^w}\left[-grad\left(p^g - p^c\right) + \rho^w\mathbf{g}\right]\right) +$$

$$+ div\left(\rho^{gw}\frac{k^{rgw}\mathbf{k}_g}{\mu^{gw}}\left[-gradp^{gw} + \rho^{gw}\mathbf{g}\right]\right) = 0$$

wsMBE

3) $$\alpha S_g div\mathbf{v}^s + \frac{nS_g}{\rho^{ga}}\dot{\rho}^{ga} + \frac{1}{\rho^{ga}}div\mathbf{J}_g^{ga} - n\dot{S}_w +$$

$$+ \frac{1}{\rho^{ga}}div\left(\rho^{ga}\frac{k^{rg}\mathbf{k}_g}{\mu^g}\left[-gradp^g + \rho^g\mathbf{g}\right]\right) - \beta_s[1-n]S_g\dot{T} = 0$$

gaMBE

4) $$\left[C_p^w nS_w\rho^w \frac{k^{rw}\mathbf{k}_w}{\mu^w}\left[-grad\left(p^g - p^c\right) + \rho^w\mathbf{g}\right] + C_p^g nS_g\rho^g\frac{k^{rg}\mathbf{k}_g}{\mu^g}\left[-gradp^g + \rho^g\mathbf{g}\right]\right]\cdot grad\,T + \left(\rho C_p\right)_{eff}\dot{T} -$$

$$div\left(\chi_{eff}\,grad\,T\right) - \rho^w\frac{nS_w}{K_w}\Delta H_{vap}\left[\dot{p}^g - \dot{p}^c\right] - \Delta H_{vap}\rho^w S_w\alpha\,\mathbf{mL\dot{u}} + \Delta H_{vap}\beta_{sw}\dot{T} - n\Delta H_{vap}\dot{S}_w\left[\rho^w - \rho^{gw}\right] -$$

$$div\left(\rho^w\frac{k^{rw}\mathbf{k}_w}{\mu^w}\left[-gradp^w + \rho^w\mathbf{g}\right]\right)\Delta H_{vap} = \boldsymbol{\sigma}'\dot{\boldsymbol{\varepsilon}}^p$$

~~EBE~~

1a- Wave propagation problem in a solid bar

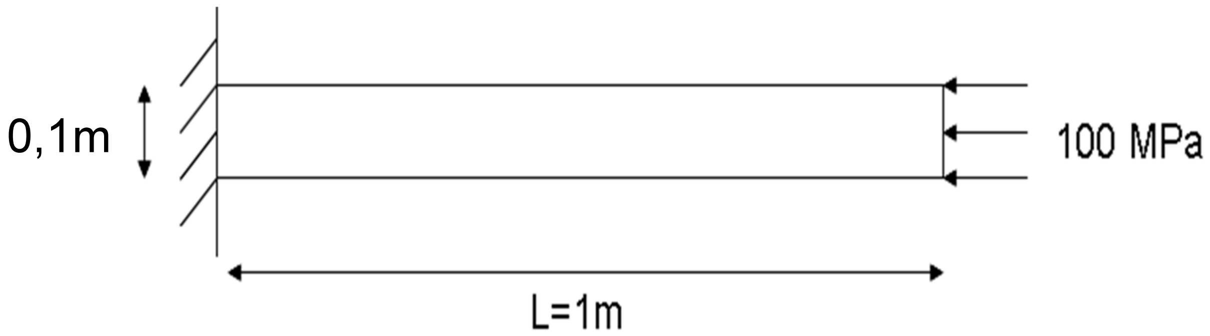

(L.J Sluys, 1992, PhD thesis)

$n=0$

$\nu = 0$

$E = 210$ GPa

$\rho = 7860$ kg/m^3 (steel)

Linear elastic solid

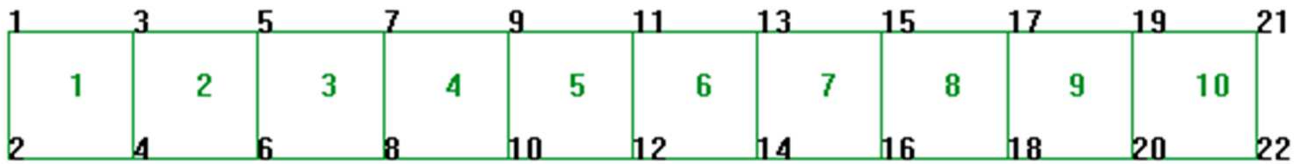

Spatial discretization (4-nodes isoparametric elements; 4 Gauss points integration)

1a- Wave propagation problem in a solid bar

Wave Velocity $V = \sqrt{\frac{E}{\rho}} = \sqrt{\frac{210E9}{7860}} = 5044 \frac{m}{s}$

Period $T = \frac{4L}{V} = \frac{1}{5044} = 7{,}93E-4s$

Axial strain $\varepsilon_x = \frac{\sigma_x}{E} = \frac{100E6}{210E9} = 0{,}47E-3$

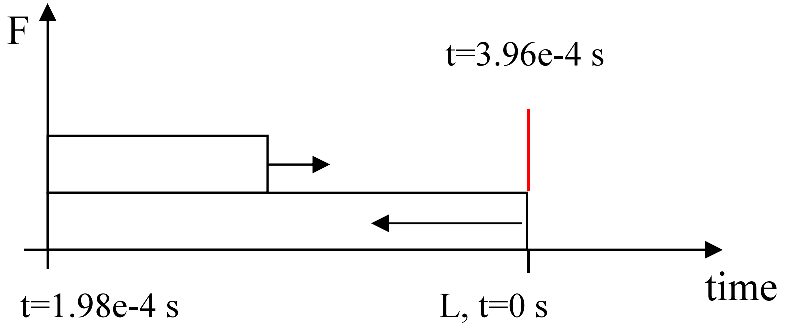

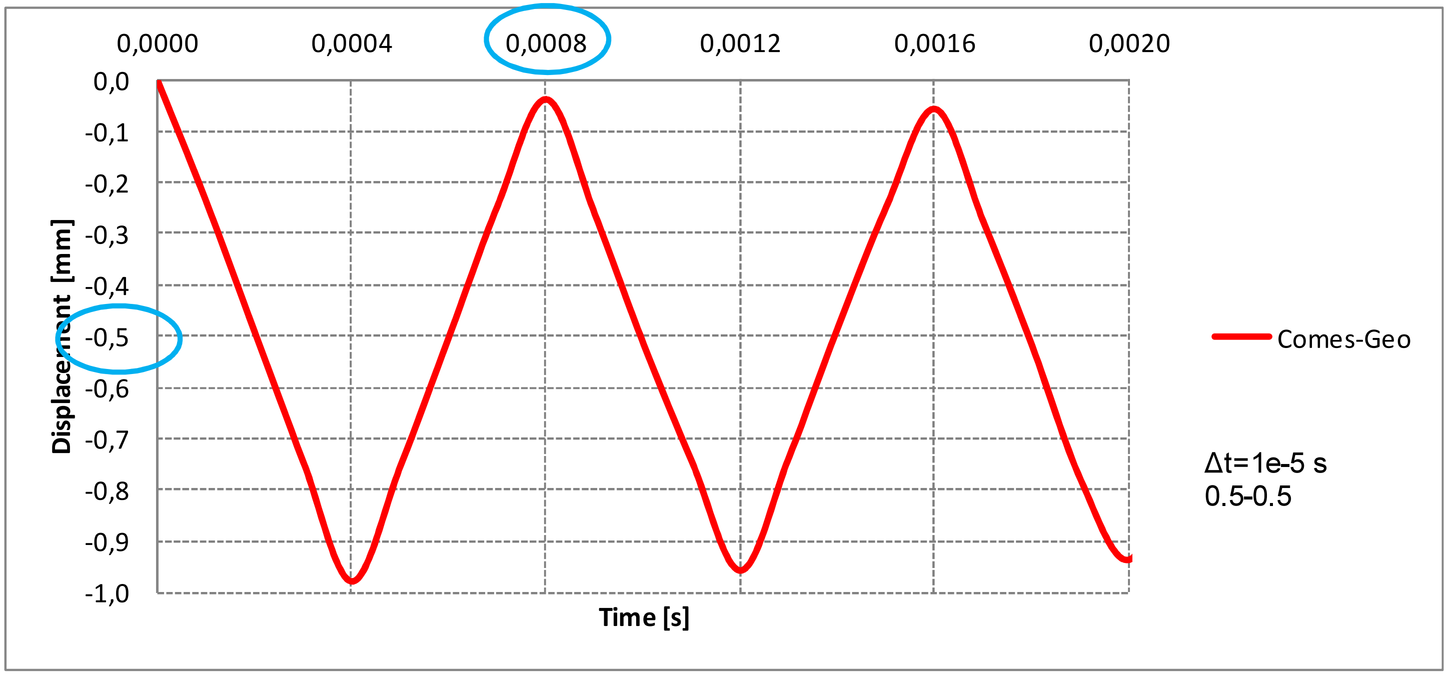

Displacement time history of the free side of the bar

1a- Wave propagation problem in a solid bar

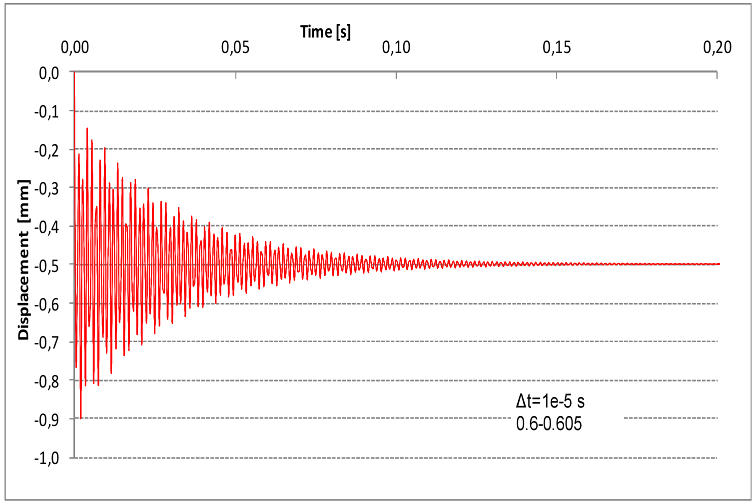

Displacement time history of the free side of the bar

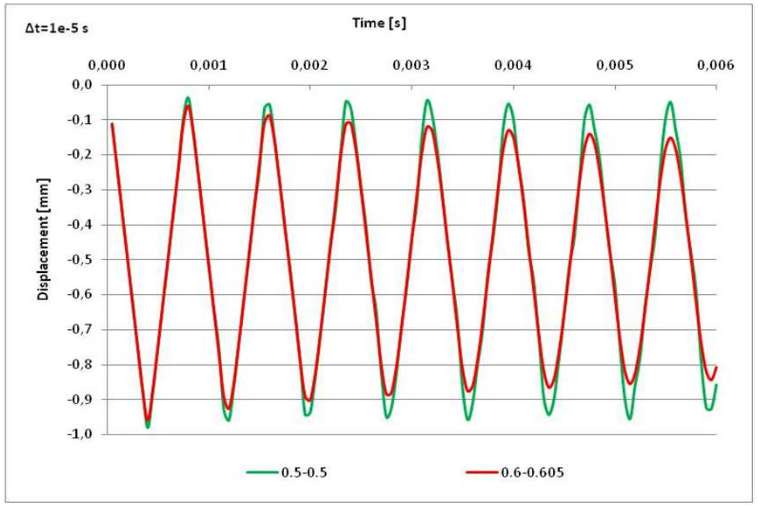

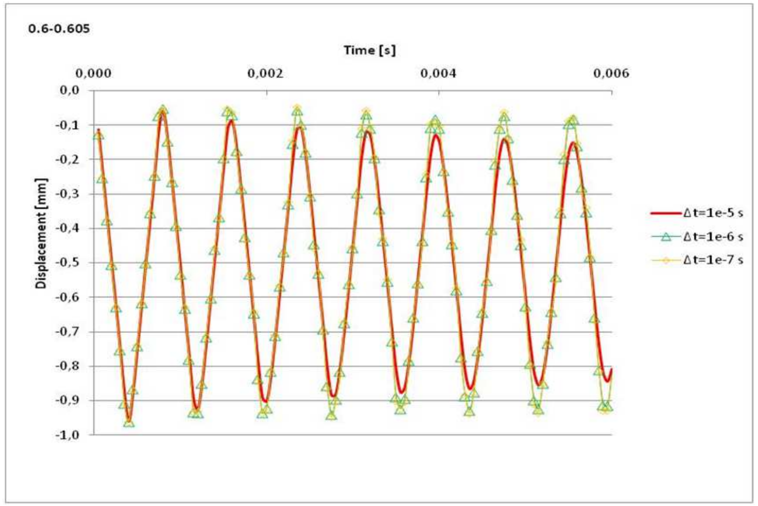

Numerical damping: comparison between different time integration parameters

Numerical accuracy: comparison between different time steps

Numerical validation (Comes-Geo fem code – Unipd, I)

http://www.dicea.unipd.it/

1. Validation of the **isothermal solid phase model**

   1a- Wave propagation problem in a solid bar - (analytical solution)

   1b- Wave propagation problem in a dry sand column (numerical comparison)

2. Validation of the **isothermal water saturated model**

   Dynamic consolidation - (analytical solution)

3. Validation of the **non-isothermal water saturated model**

   Non-isothermal consolidation - (Aboustit et al. numerical test)

4. Validation of the **isothermal variably saturated model**

   4a- Liakopoulos test: quasi-static drainage of liquid water from an initially water saturated sand column - (numerical benchmark)

   4b- Unsaturated sand column subjected to a step load (numerical comparison)

2- Dynamic consolidation in <u>water saturated</u> elastic column under harmonic load

(B. Markert, 2010, Habilitation thesis, Universitaet Stuttgart)

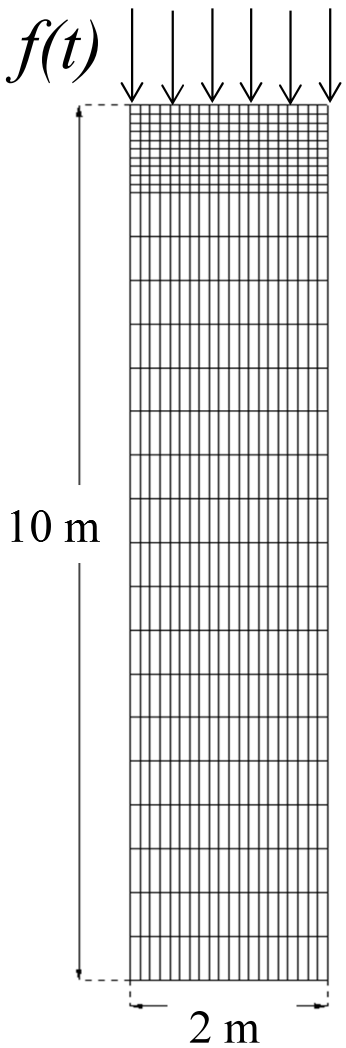

Initial condition	
P^g = Patm	fixed
P^c = 0,0	
T = 293.15 °K	fixed
u_x = 0.0	on the lateral nodes
u_y = 0.0	on the bottom

Boundary condition	
P^g = Patm	fixed
P^c = 0.0	at the top
T = 293.15 K	fixed
u_x = 0.0	on the lateral nodes
u_y = 0.0	on the bottom

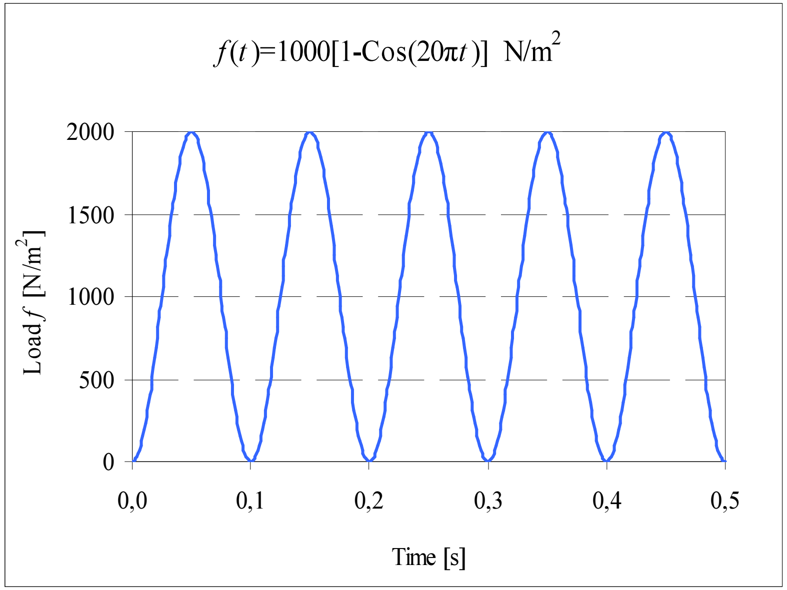

Material parameters		Value	SI unit
Young's Modulus	E	1,45E+07	Pa
Poisson's Modulus	ν	0,3	-
Porosiy	n	0,33	-
Density of the solid	ρ	2000	kg/m^3
Gravity acceleration	g	0	m/s^2
Permeability	k_w	10^{-2};10^{-5}	m/s

Incompressible liquid water

Spatial discretization (8-node isoparametric elements; 9 Gauss points integration)

2- Dynamic consolidation in water saturated elastic column under harmonic load

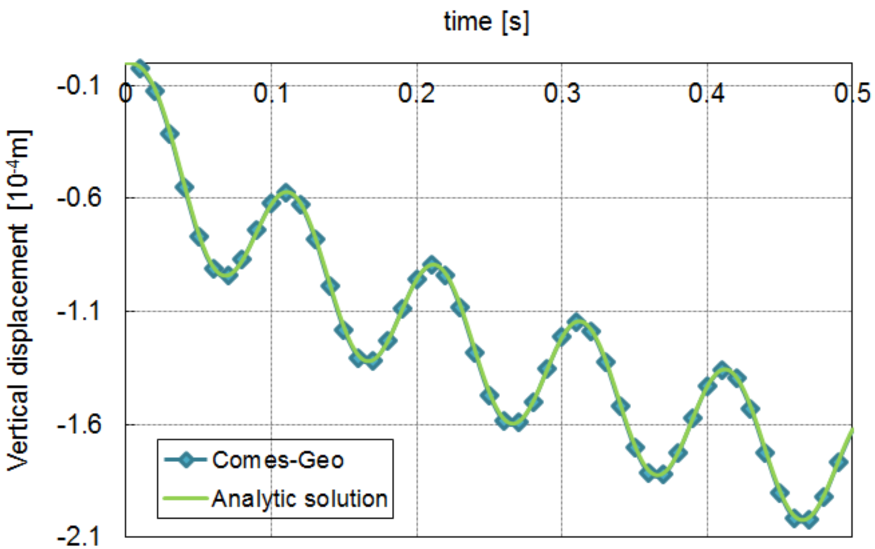

a)

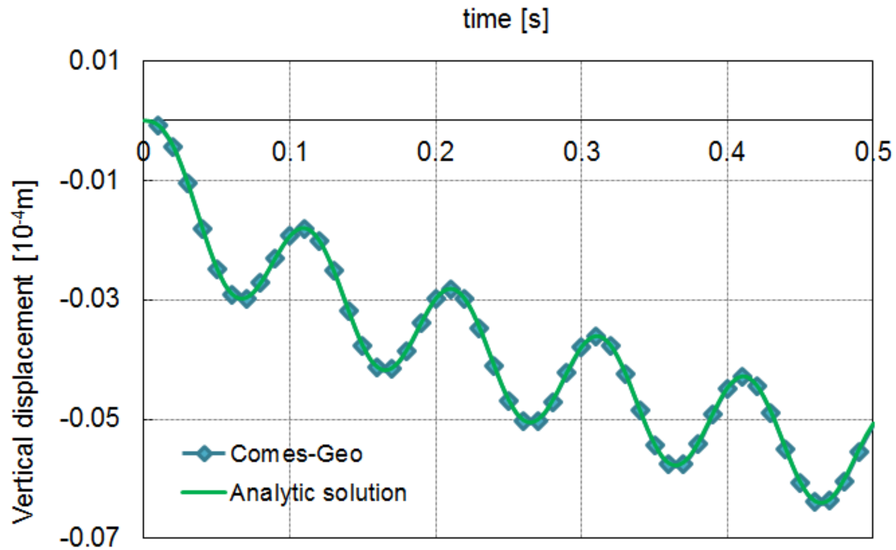

b)

Displacement history, top surface

a) k_w =10^{-2} m/s, b) k_w =10^{-5} m/s

Analytical solution: de Boer, 1993, Arch. Appl. Mech.

Numerical validation (Comes-Geo fem code – Unipd, I)

http://www.dicea.unipd.it/

1. Validation of the **isothermal solid phase model**

   1a- Wave propagation problem in a solid bar - (analytical solution)

   1b- Wave propagation problem in a dry sand column (numerical comparison)

2. Validation of the **isothermal water saturated model**

   Dynamic consolidation - (analytical solution)

3. Validation of the **non-isothermal water saturated model**

   Non-isothermal consolidation - (Aboustit et al. <u>numerical test</u>)

4. Validation of the **isothermal variably saturated model**

   4a- Liakopoulos test: quasi-static drainage of liquid water from an initially water saturated sand column - (numerical benchmark)

   4b- Unsaturated sand column subjected to a step load (numerical comparison)

3- Non-isothermal consolidation in a water saturated elastic column

Numerical solution: Sanavia et al. JTAM 2008 (quasi-static) - Aboustit et al. NAG 1985

$f(t) = 10000$ Pa

$\Delta t = 50$ K

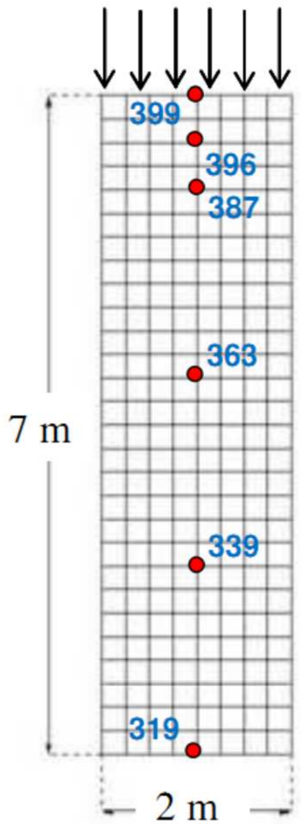

Initial condition	
P^g = Patm	fixed
P^c = idrostatic	
T = 293.15 K	fixed
u_x = 0.0	on the lateral nodes
u_y = 0.0	on the bottom

Boundary condition	
P^g = Patm	fixed
P^c = 0.0	at the top
T	not fixed
u_x = 0.0	on the lateral nodes
u_y = 0.0	on the bottom

Material parameters		Value	SI unit
Porosity	n	0,39	-
Intrinsic permeability	k	2,0 E-19	m^2
Solid skeleton density	ρ_s	2670	kg/m3
Irreducible saturation point	S_{irr}	0,05	-
Solid thermal conductivity		0,42	W/(m K)
Solid matrix heat conductivity		1,9 E-16	W/(m K)
Solid specific heat		732	J/(kg K)
Cubic thermal expansion coefficient		1,3 E-5	K^{-1}
Biot's constant	α_B	1	-

Spatial discretization (8-node isoparametric elements; 9 Gauss points integration)

3- Non-isothermal consolidation in a water saturated elastic column

Numerical solution: Sanavia et al. JTAM 2008 (quasi-static) - Aboustit et al. NAG 1985

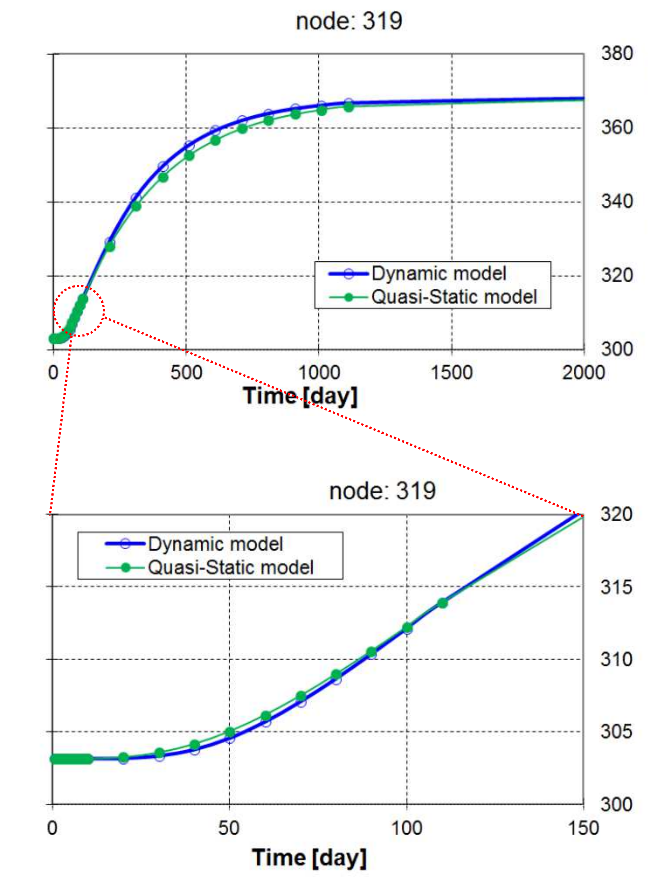

Temperature time history
(bottom surface)

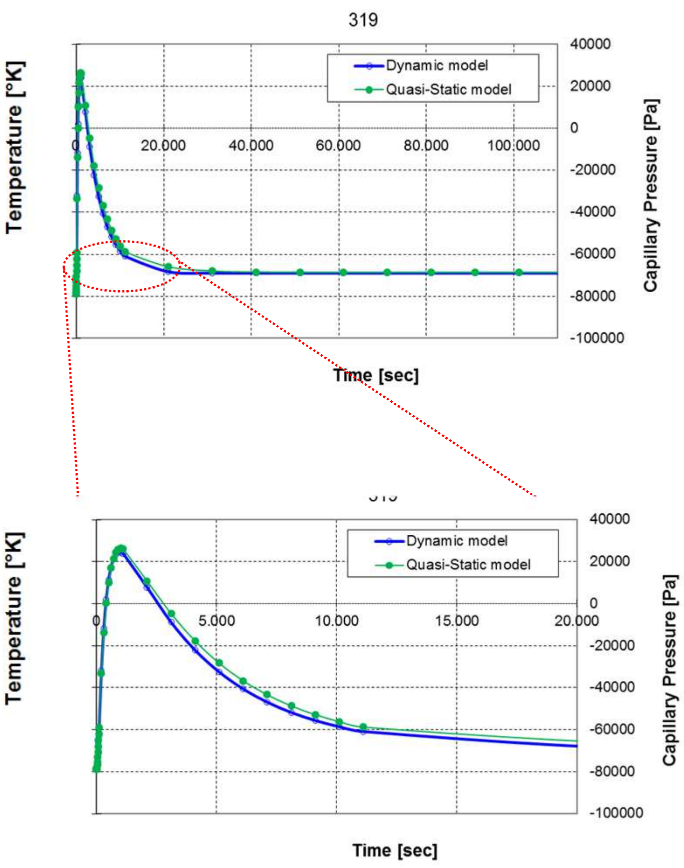

Capillary pressure time history
(bottom surface)

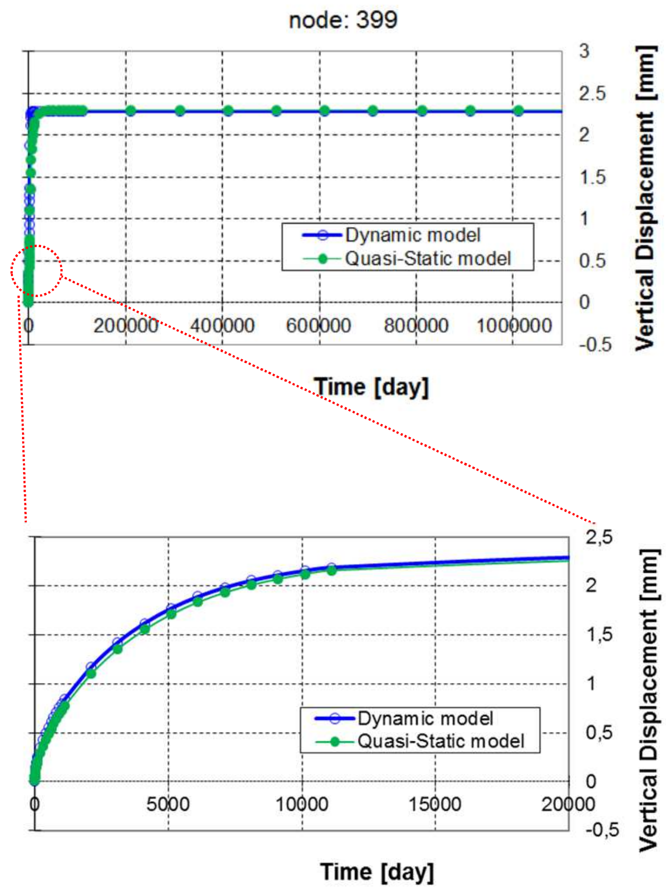

Displacement time history
(top surface)

Numerical validation (Comes-Geo fem code – Unipd, I)

http://www.dicea.unipd.it/

1. Validation of the **isothermal solid phase model**

    1a- Wave propagation problem in a solid bar - (analytical solution)

    1b- Wave propagation problem in a dry sand column (numerical comparison)

2. Validation of the **isothermal water saturated model**

    Dynamic consolidation - (analytical solution)

3. Validation of the **non-isothermal water saturated model**

    Non-isothermal consolidation - (Aboustit et al. numerical test)

4. Validation of the **isothermal variably saturated model**

    4a- Liakopoulos test: quasi-static drainage of liquid water from an initially water saturated sand column - (numerical benchmark)

    4b- Unsaturated sand column subjected to a step load (numerical comparison)

4a- Drainage of water from a soil column: Liakopoulos test - isothermal variably saturated model

(Liakopoulos, PhD thesis, 1965, University of California-Berkeley)

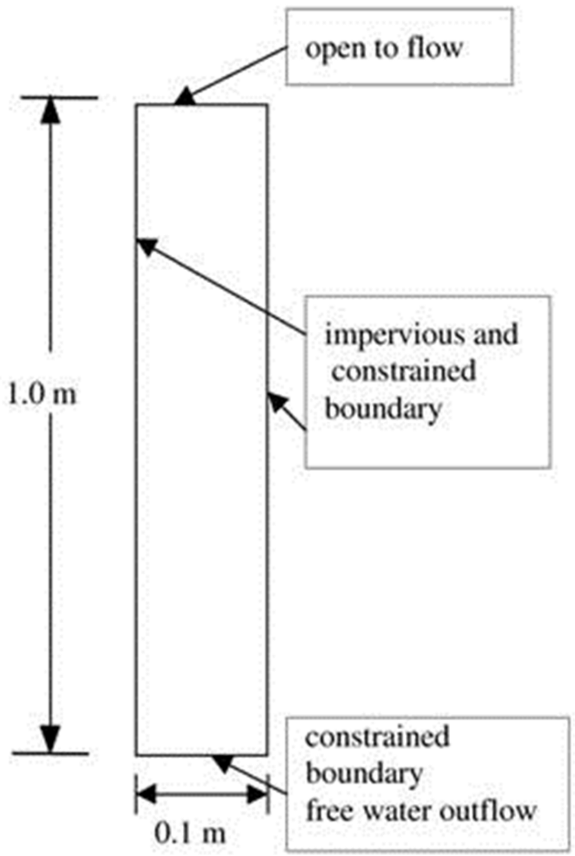

Initial condition	
P^g = Patm	on the top
P^c = idrostatic	
T = 293.15 K	fixed
u_x = 0.0	on the lateral nodes
u_y = 0.0	on the bottom

Boundary condition	
P^g = Patm	on the top, on the bottom
P^c = 0.0	on the bottom
T = 293.15 K	fixed
u_x = 0.0	on the lateral nodes
u_y = 0.0	on the bottom

Numerical solution:

Gawin and Schrefler EC 1995

(quasi-static)

Gawin and Sanavia CMES 2009

Material parameters		Value	SI unit
Porosity	n	0,2975	-
Intrinsic permeability	k	4,5 E-13	m^2
Solid skeleton density	ρ_s	2000	kg/m^3
Irreducible saturation point	S_{irr}	0,2	-
Critical saturation point	S_{cri}	0,909	-
Young's modulus	E	1,3 E+06	Pa
Poisson's coefficient	ν	0,4	-
Biot's constant	α_B	1	-
Bulk modulus of water	Kw	2,2 E+09	Pa

Spatial discretization (8-node isoparametric elements; 9 Gauss points integration)

4a- Drainage of water from a soil column: Liakopoulos test

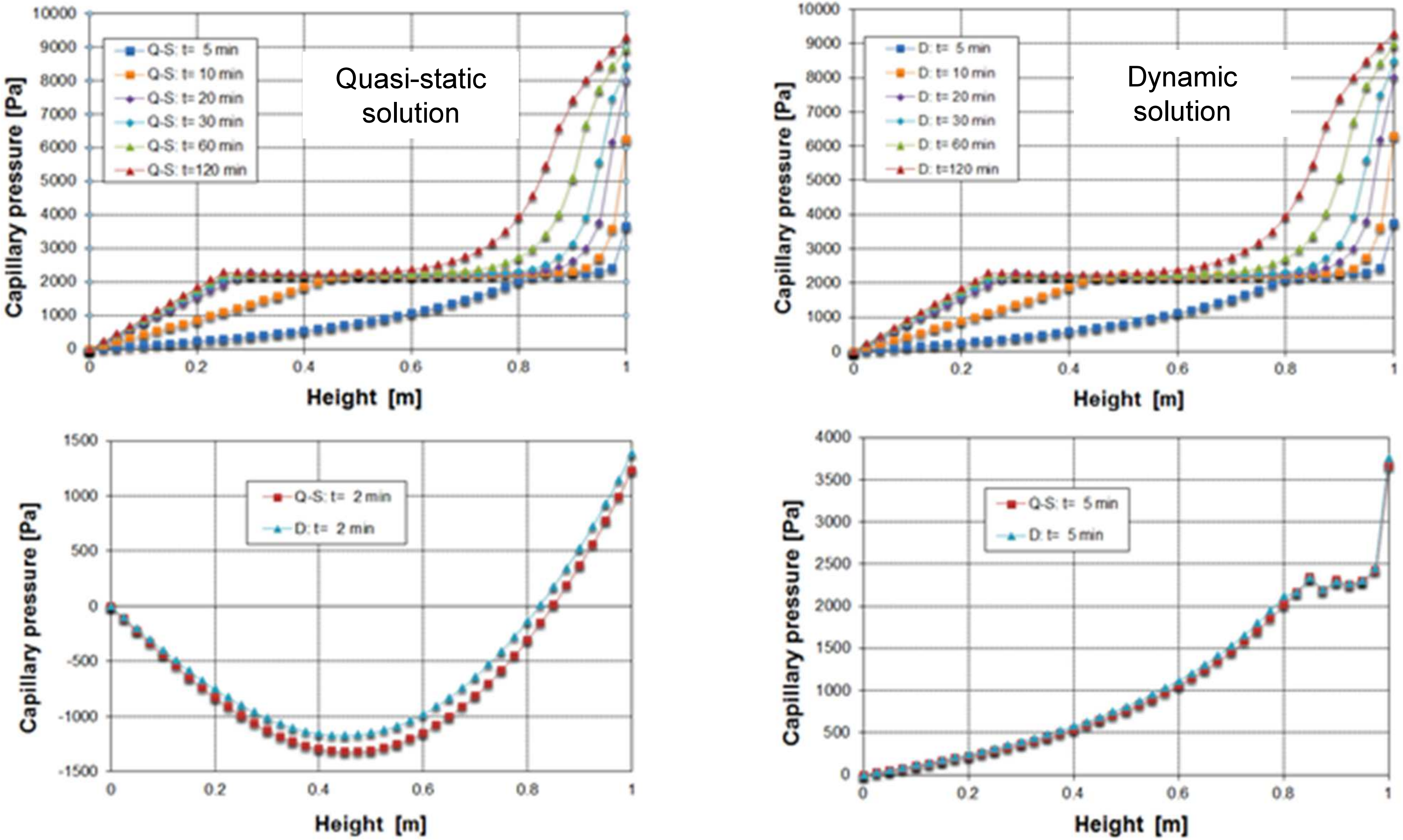

Comparison between quasi-static and dynamic solution

4a- Drainage of water from a soil column: Liakopoulos test

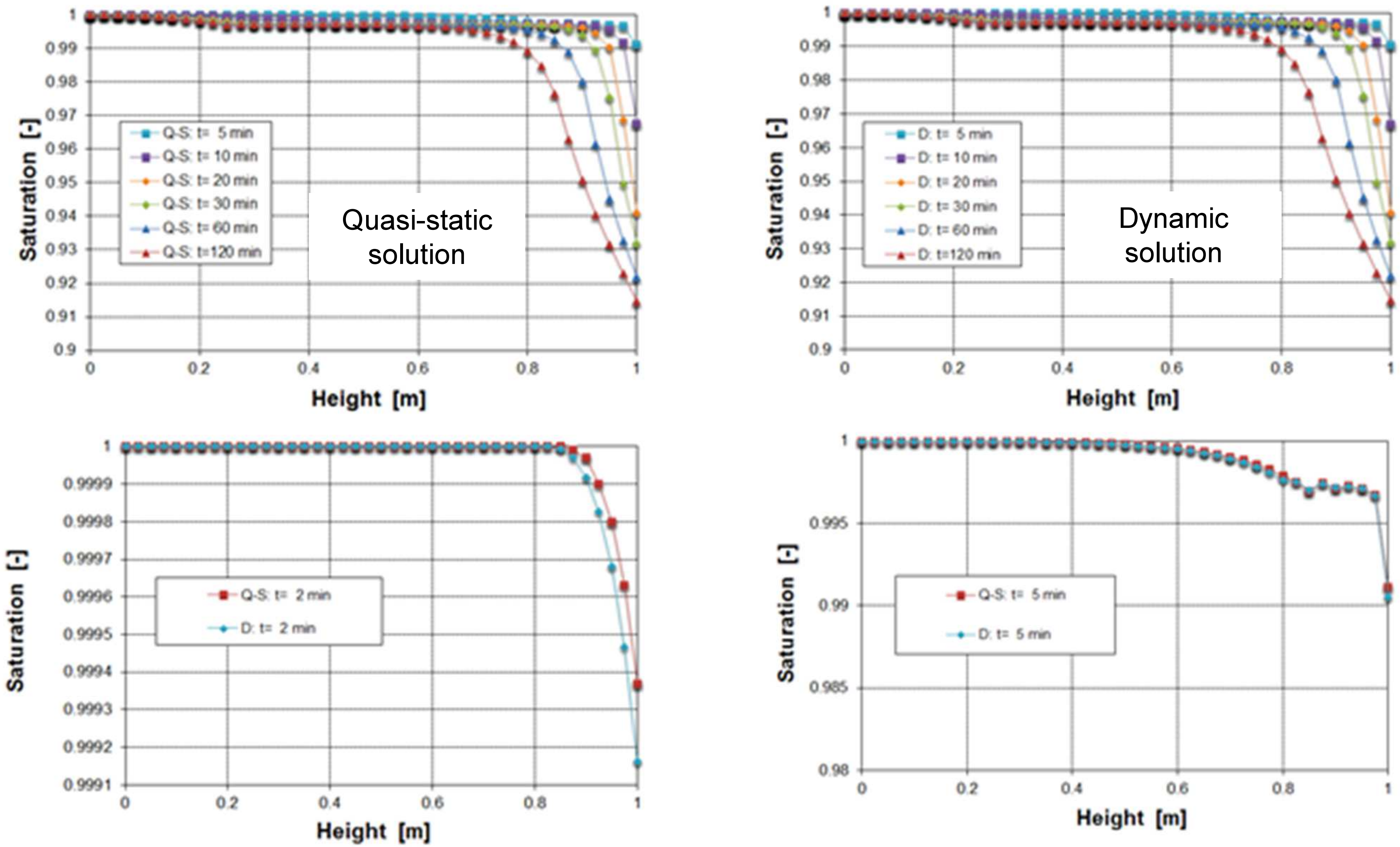

Comparison between quasi-static and dynamic solution

Biaxial compression test of initially water saturated globally undrained dense Hostun sands

Desrues & Mokni (Grenoble - Fr 1992, *MCF 4 1998*)

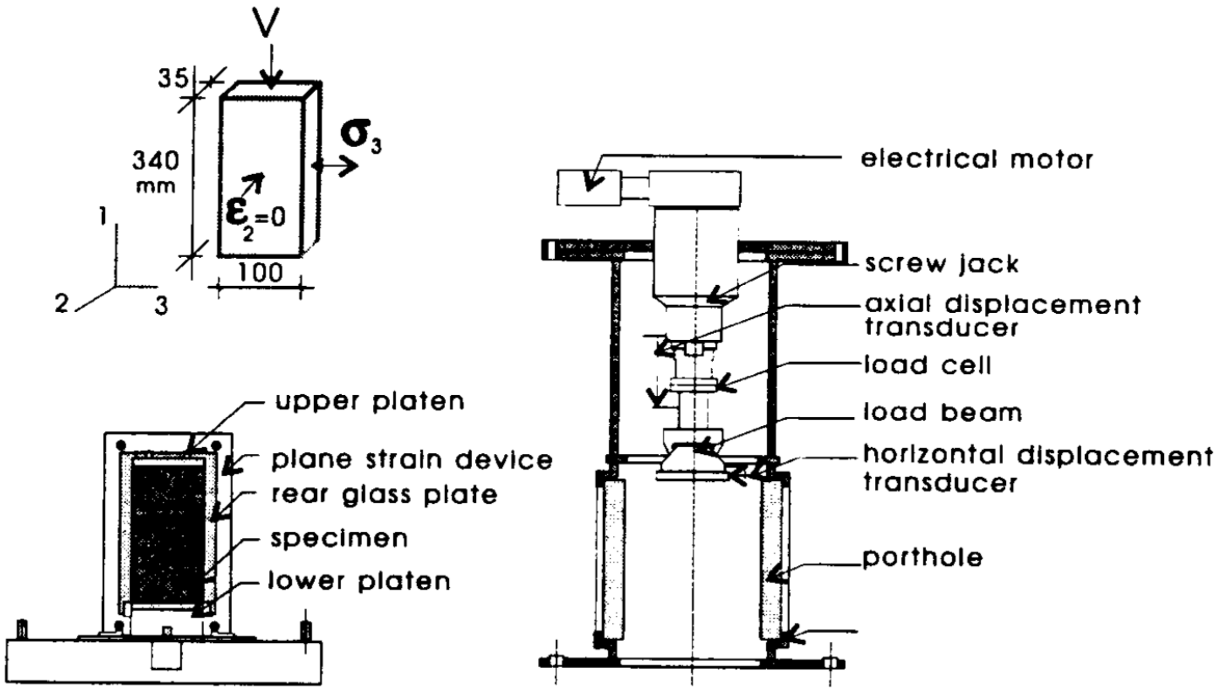

plane strain device
and specimen

pressure cell
and loading device

biaxial compression test on Hostun sands

Biaxial compression test of initially water saturated globally undrained dense Hostun sands

Desrues & Mokni (Grenoble – Fr, 1992, MCF 1998)

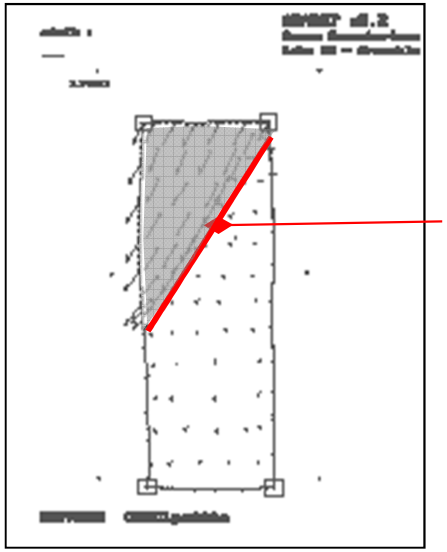

Failure plane

Failure

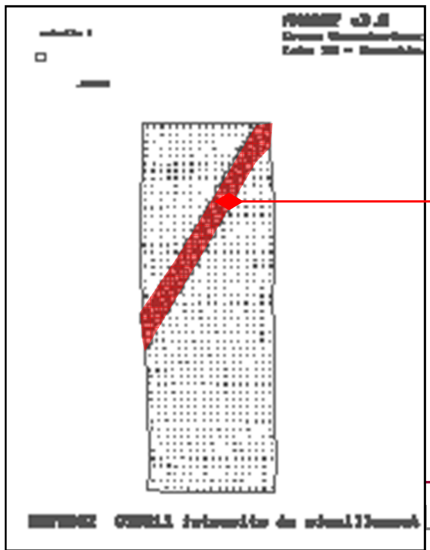

Dilatant shear band

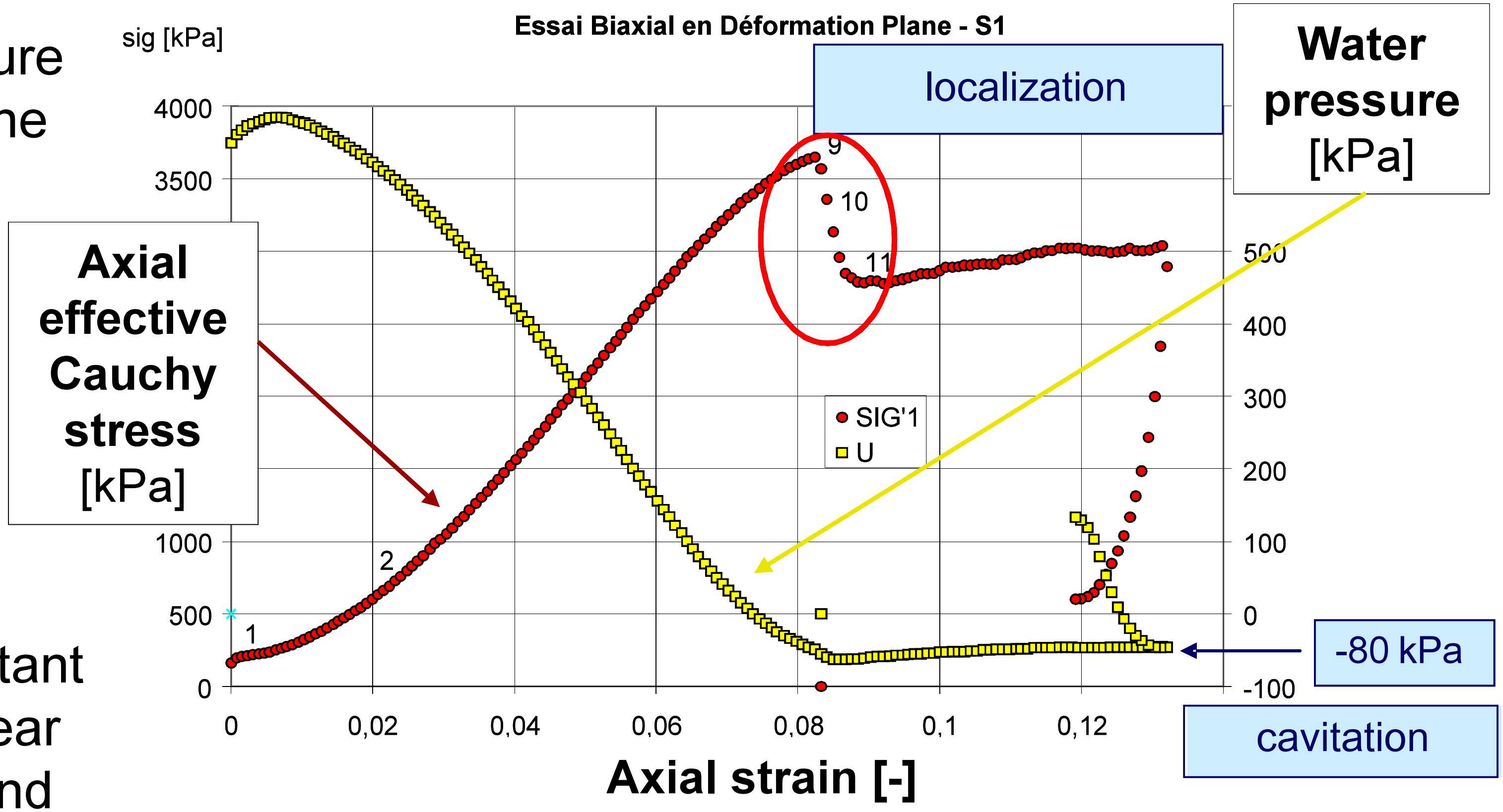

• Experimental conditions: de-aired water

Strain localization in globally undrained dense sand

- ✓ K_w=2.2e9 Pa & Velocity of wave propagation = 1483.24 m/s
  - ❑ $T_{crit} = \frac{Length}{Velocity}$ =0.00023 s
- ✓ The time for analysis of dynamic problems
  - ❑ $\Delta t \leq T_{crit}$=0.00023 s

Imposed vertical displacements
(**1.2** & **2.4** & **3.6** & **6 mm/s**)

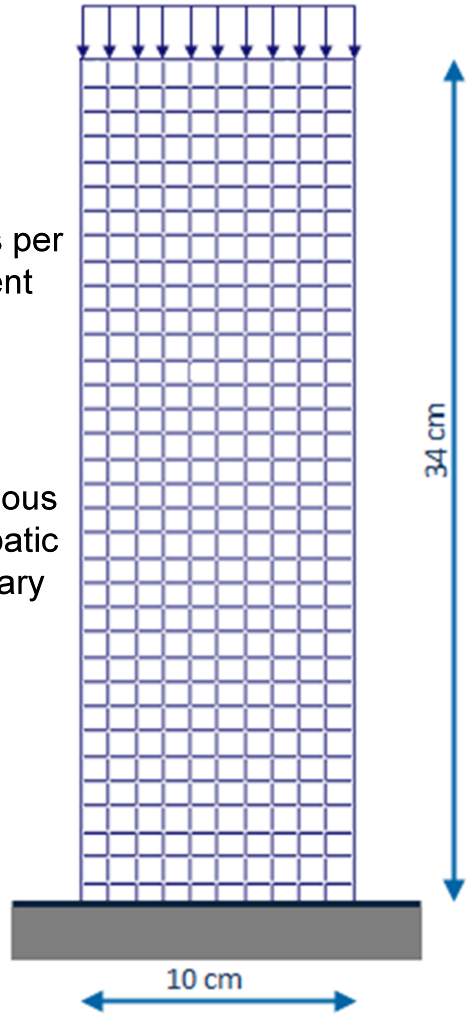

Material parameters

Young modulus	E = 30 MPa	linear softening modulus	h = -1.0 MPa
Poisson ratio	ν = 0.4	Initial porosity	n_0 = 0.20
Gravity acceleration	g = 9.81 m/s^2	Initial intrinsic permeability	k = 1.0E-14 m^2
Initial apparent cohesion	c_0 = 0.5 MPa	Water unit weight	γ_w = 10 kN/m^3
Angle of internal friction	ϕ = 30°	Solid density	ρ^s = 2000 kg/m^3
Dilatancy angle	ψ = 20°	Drucker-Prager model	

(Sanavia et al., 2006 - inspired by Mokni and Desrues, 1998)

Strain localization in globally undrained dense sand

- Velocity load = 0.0024 m/s

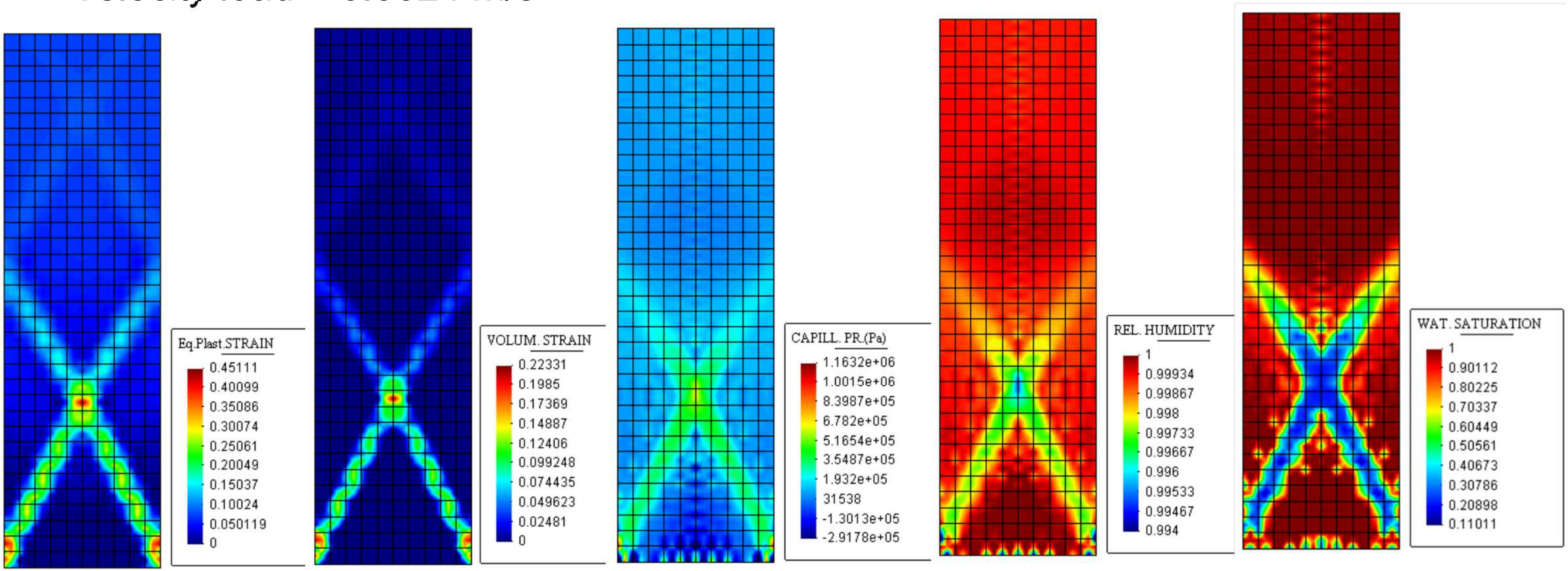

Equivalent plastic strain [-], volumetric strain [-], capillary pressure [Pa], relative humidity [-] and saturation degree[-] contours at 19 s

Crucial issue in shear band modelling: objectivity of FE results

Strain localization is a material instability phenomenon

$d_2 w = d\sigma : d\varepsilon < 0$ (Hill 1958) $d_2 w^p = d\sigma : d\varepsilon^p < 0$ (Drucker 1951)

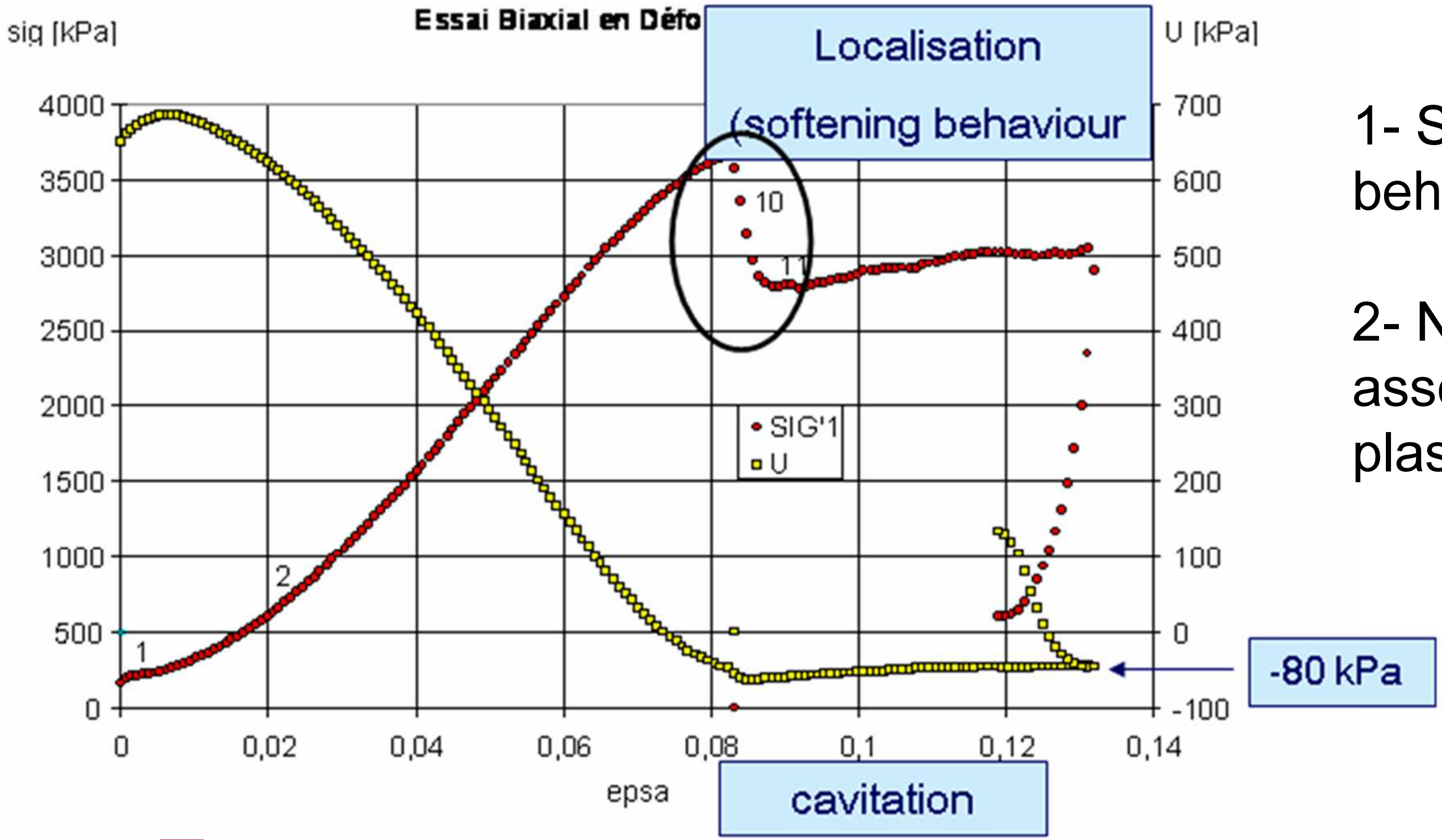

1- Softening behaviour

2- Non-associated plastic flow

Crucial issue: objectivity of FE results

Strain softening single phase materials – von Mises plasticity

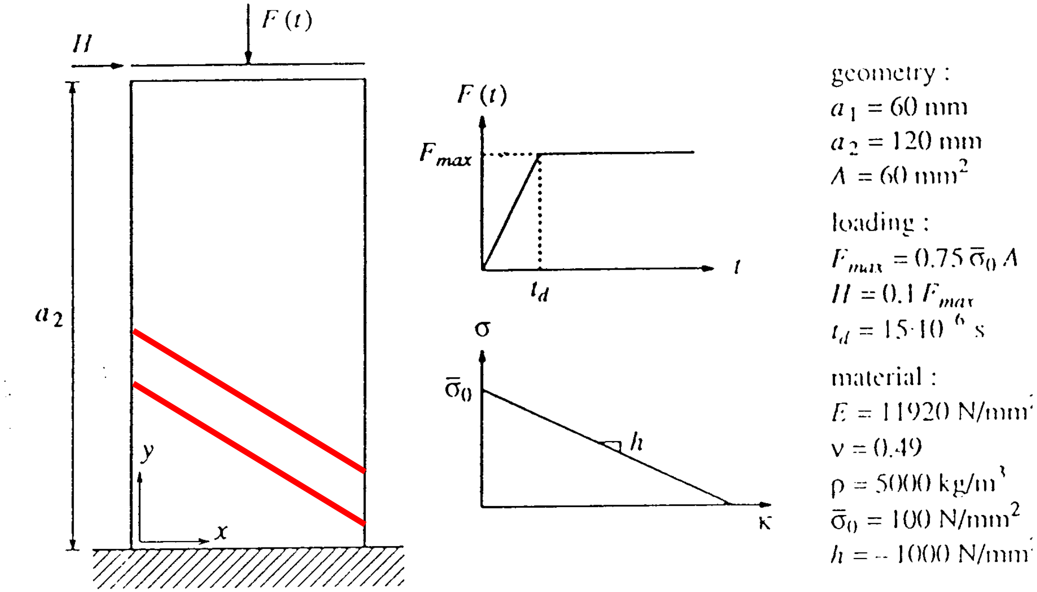

Fig. 3.14: Impact biaxial test

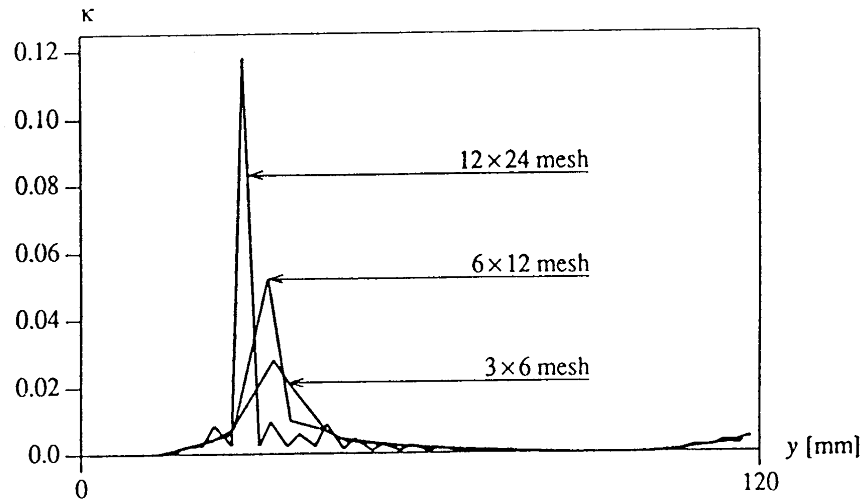

Fig. 3.17: Equivalent plastic strain in centre section of the sample (t=0.1275E-3 s)

L.J. Sluys, PhD thesis, 1992: "Wave propagation, localisation and dispersion in softening solids" – Delft University of Technology

1. F.E. dimension sets shear band width
2. maximum level of effective plastic strain inside shear band is inversely proportional to F.E. dimension

Strain-softening single phase continuum

- **Dynamics**: when strain softening occurs, domain splits into an elliptic part with imaginary wave speed (standing wave) and hyperbolic part where waves can propagate

(**Cauchy continuum**)

$$\operatorname{div}\sigma + \rho\mathbf{g} = \rho\ddot{\mathbf{u}} \quad \rightarrow \quad 1D \quad \frac{\partial \sigma}{\partial x} + \rho g = \rho \ddot{u} \quad \rightarrow \quad \frac{\partial}{\partial t}; \quad \frac{\partial \dot{\sigma}}{\partial x} = \rho \frac{\partial^2 v}{\partial t^2}$$

where $v = \dfrac{\partial u}{\partial t}$

$\dot{\varepsilon} = \dot{\varepsilon}^e + \dot{\varepsilon}^p$; small strain, linear elasto-plasticity $\dot{\sigma} = h\dot{\varepsilon}^p = E\dot{\varepsilon}^e \rightarrow \dot{\sigma} = \dfrac{Eh}{E+h}\dot{\varepsilon}$

with h = plastic modulus (h<0 **softening**)

$$\frac{\partial}{\partial x}; \quad \dot{\varepsilon} = \frac{\partial v}{\partial x} \quad \rightarrow \quad \frac{\partial^2 v}{\partial t^2} = \frac{Eh}{E+h}\frac{1}{\rho}\frac{\partial^2 v}{\partial x^2}$$

wave equation for 1D strain hardening/softening continuum

Strain-softening single phase continuum

$$\frac{\partial^2 v}{\partial t^2} = \frac{Eh}{E+h}\frac{1}{\rho}\frac{\partial^2 v}{\partial x^2}, \qquad \left(\text{with} \quad D^{ep} = \frac{Eh}{E+h}\right) \qquad c_f = \pm\sqrt{\frac{Eh/(E+h)}{\rho}}$$

wave equation for 1D elasto-plastic continuum

phase velocity

when $h<0, \quad E+h>0 \quad \rightarrow \quad c_f$ is imaginary

- **Dynamics**: when strain softening occurs, domain splits into an elliptic part with imaginary wave speed (standing wave) and hyperbolic part where waves can propagate.

- Because of the inability of the standing wave to propagate, localization zone has zero thickness with no energy consumption; against experimental evidence.

Strain-softening single phase continuum

- When F.E. models tries to simulate strain <u>softening</u>, the first plastic wave is <u>unable to propagate</u> and locks.

- When the mesh is refined, the shear band width decreases

$\Rightarrow$ pathologic <u>mesh dependence</u>.

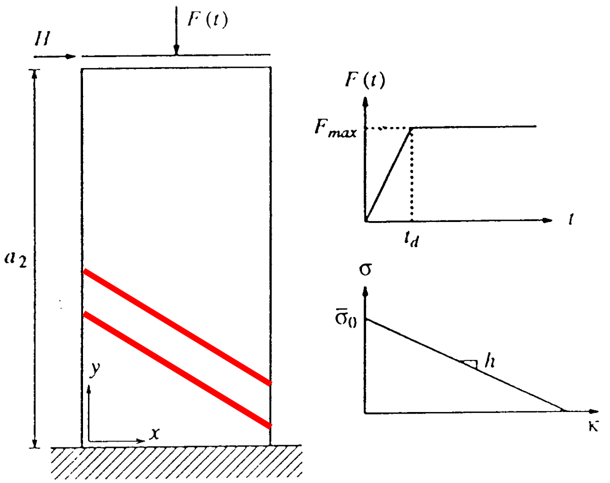

geometry :
$a_1 = 60$ mm
$a_2 = 120$ mm
$A = 60$ mm^2

loading :
$F_{max} = 0.75\,\bar{\sigma}_0\,A$
$H = 0.1\,F_{max}$
$t_d = 15 \cdot 10^{-6}$ s

material :
$E = 11920$ N/mm^2
$\nu = 0.49$
$\rho = 5000$ kg/m^3
$\bar{\sigma}_0 = 100$ N/mm^2
$h = -1000$ N/mm^2

Fig. 3.14: Impact biaxial test

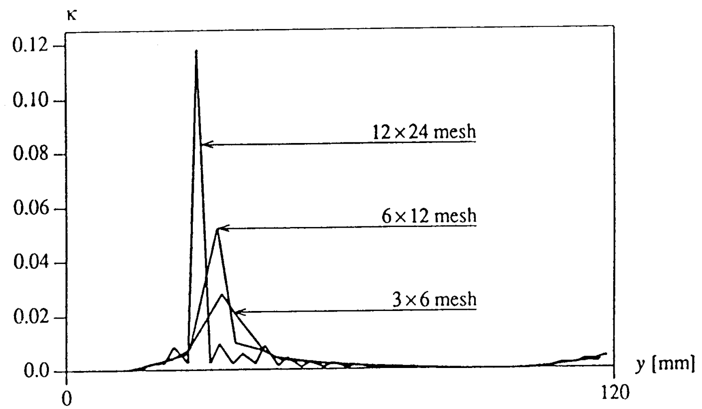

Fig. 3.17: Equivalent plastic strain in centre section of the sample (t=0.1275E-3 s)

L.J. Sluys, PhD thesis, 1992: “Wave propagation, localisation and dispersion in softening solids” – Delft University of Technology

Crucial issue: objectivity of FE results

- (Cauchy continuum) isothermal rate-independent single phase material model does not contain any internal length scale to set shear band width.

- To maintain hyperbolicity in dynamics (or ellipticity in quasi-static problems), we need to regularize the governing equations:

  - inclusion of gradient or Laplacian term (higher-order gradient terms; e.g. non-local strain models, 2nd-order gradient of internal variables, etc.)

  - inclusion of rate-dependent term (extra higher-order time derivative terms; e.g. visco-plasticity),

  - inclusion of rotational degrees of freedom (micro-polar Cosserat model).

Crucial issue: objectivity of FE results

- All these models introduce implicitly or explicitly an internal length scale for strain localization analysis.

- Multi-phase porous media models contain a Laplacian in the mass balance eq. of the fluids if Darcy's law is introduced:

Mass balance equation (solid + liquid + vapour):

$$n[\rho^w - \rho^{gw}]\frac{\partial S_w}{\partial t} + [\rho^w S_w + \rho^{gw} S_g] div\left(\frac{\partial \boldsymbol{u}}{\partial t}\right)$$
$$+ nS_g\frac{\partial \rho^{gw}}{\partial t} - div\left(\rho^g \frac{M_a M_w}{M_g^2}\boldsymbol{D}_g^{gw} grad\left(\frac{p^{gw}}{p^g}\right)\right)$$
$$+ div\left(\rho^{gw}\frac{\boldsymbol{k}\, k^{rg}}{\mu^g}[-grad\,(p^g) + \rho^g \boldsymbol{g}]\right) - \beta_{swg}\frac{\partial T}{\partial t}$$
$$+ div\left(\rho^w\frac{\boldsymbol{k}\, k^{rw}}{\mu^w}[-grad\,(p^g) + grad\,(p^c) + \rho^w \boldsymbol{g}]\right) = 0$$

Crucial issue: objectivity of FE results

- The **dynamic** equations for variably saturated geomaterials *may* remain hyperbolic even after the onset of strain softening and an internal length scale can be defined:

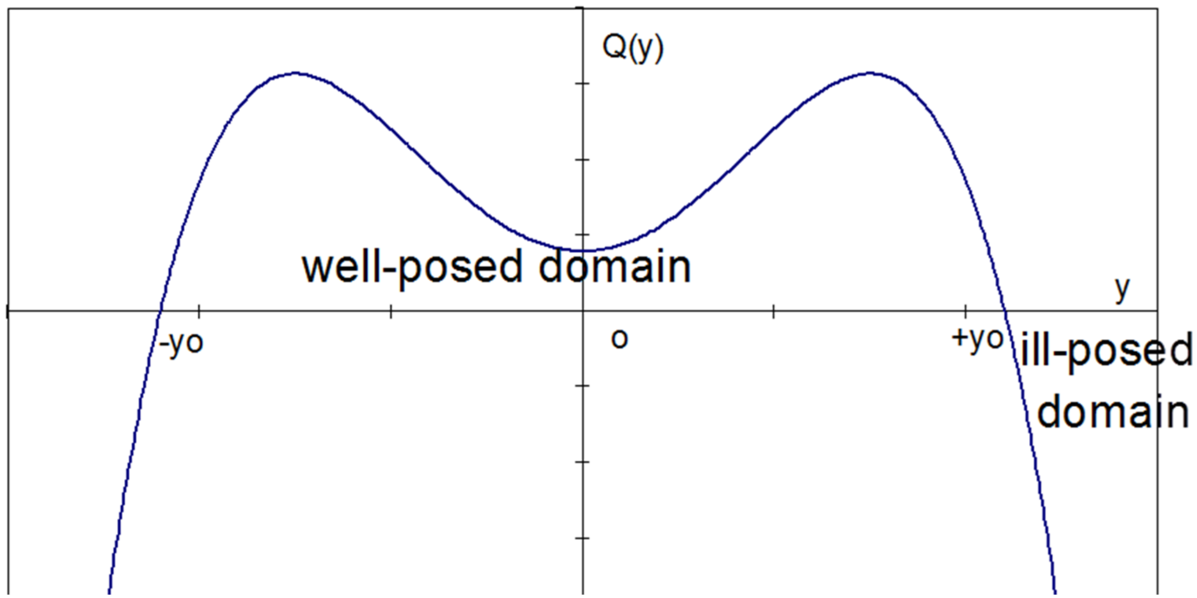

Distribution of the wave number domains for fully and partially saturated geomaterials

- For the “**quasi-static**” case, this internal length cannot be defined and a regularization strategy has to be used.

Strain localization in globally undrained dense sand

Drucker-Prager elasto-plasticity – multiphase porous media in dynamics

(*Cao, Sanavia, Schrefler, NME under revision*)

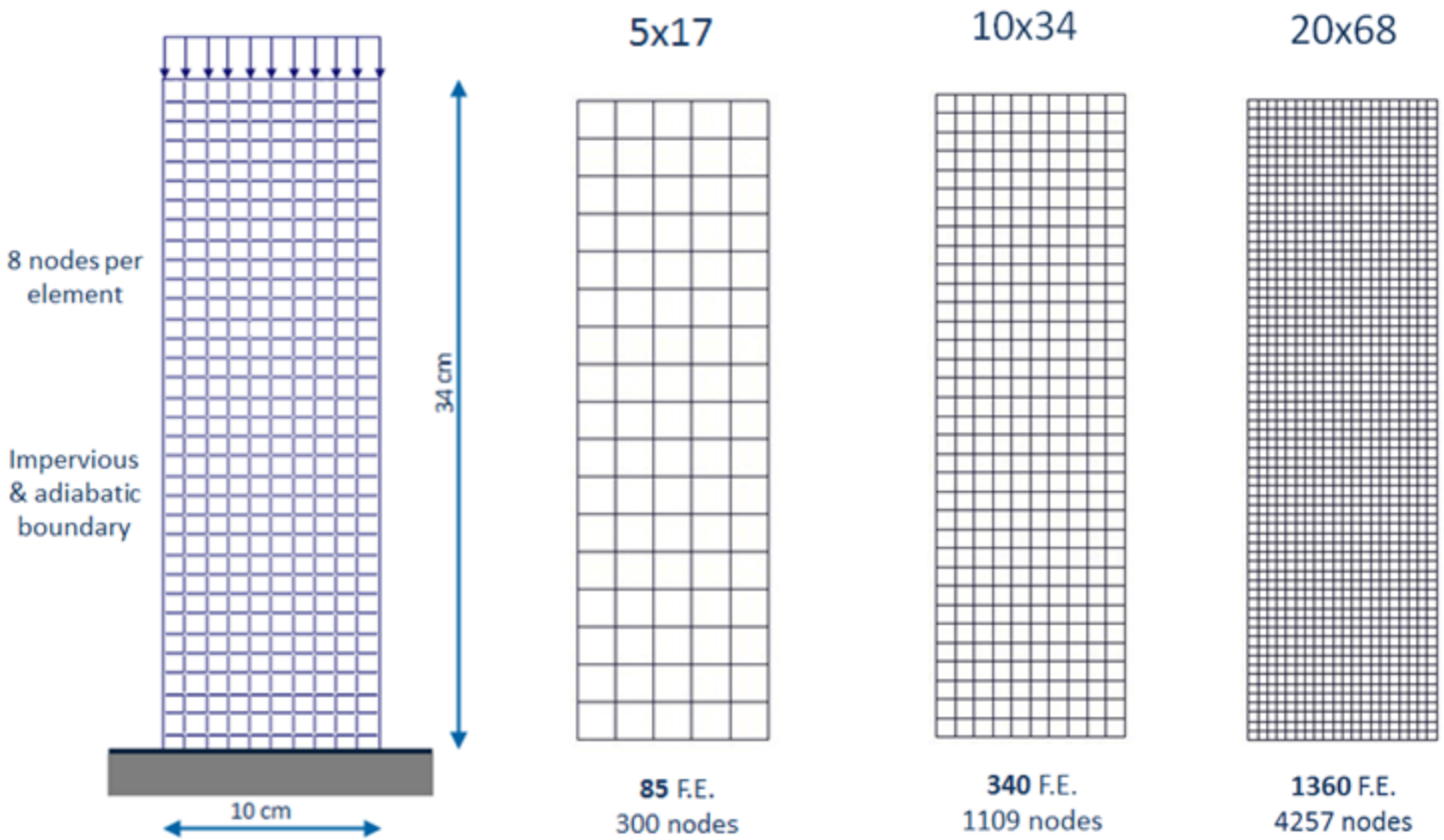

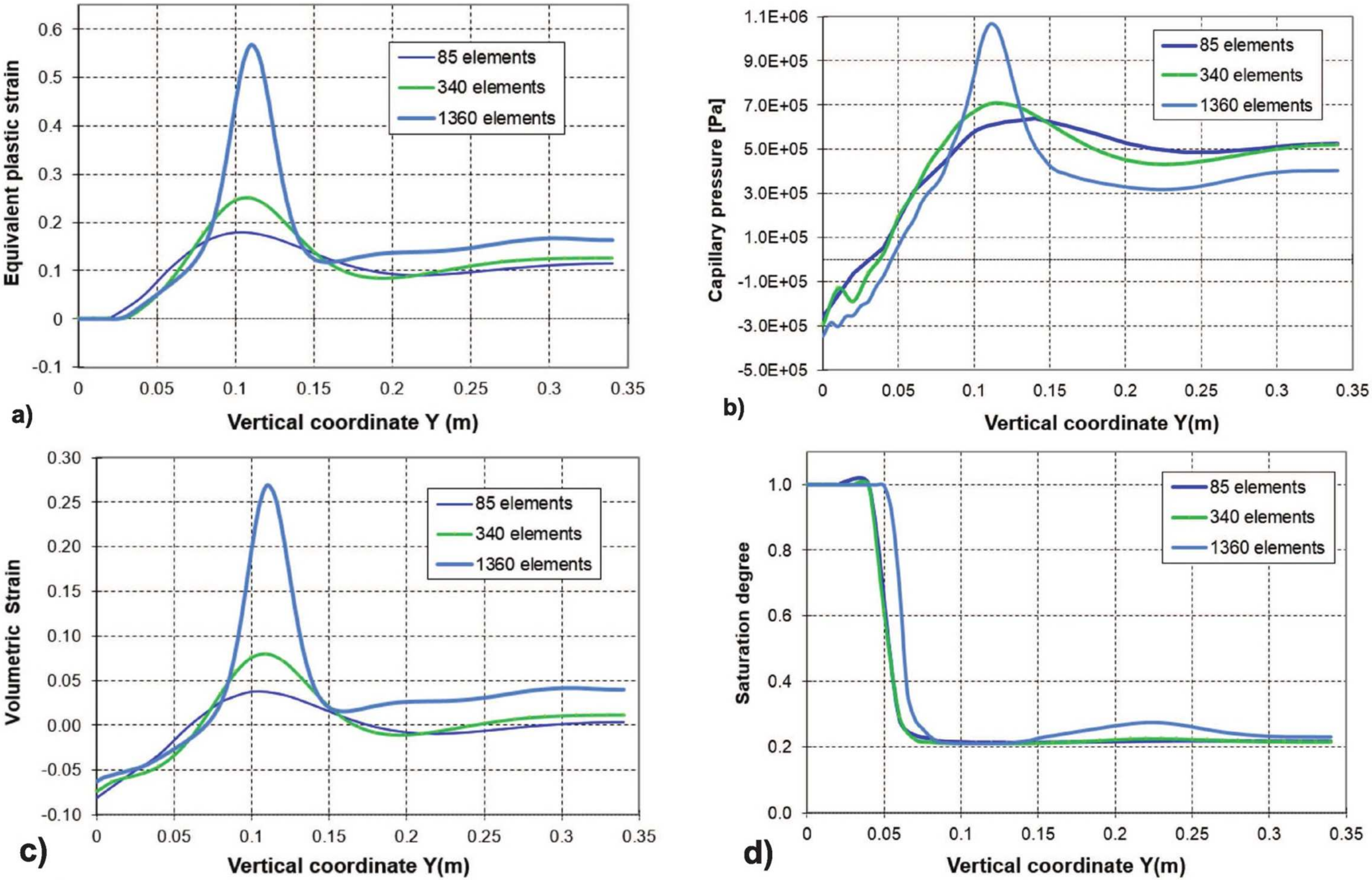

Numerical results, vertical section in the middle of the sample, with 3 different meshes (85, 340, 1360 F.E.) - (Cao, Sanavia, Schrefler, NME under revision)

FEM regularization for post localized bifurcation

Visco-plasticity as regularization strategy

Perzyna model (1966) - (in cooperation with Maria Lazari)

Drucker-Prager yield surface with non associative flow rule & linear isotropic hardening (*Sanavia et al., 2006*):

$$F\left(p,\mathbf{s},\xi\right)=3\alpha_n p+\|\mathbf{s}\|+\beta_n\sqrt{\frac{2}{3}}\left[c_0+h\xi\right]$$

$$\alpha_n=2\frac{\sqrt{\frac{2}{3}}\sin\varphi}{3\text{-}\sin\varphi},\qquad \beta_n=\frac{6\cos\varphi}{3\text{-}\sin\varphi}$$

p: mean Cauchy pressure

s: deviator Cauchy stress tensor

ξ: equivalent viscoplastic strain

c_0: initial cohesion

h: hardening/softening modulus

MUMOLADE

FEM regularization for post localized bifurcation

Visco-plasticity as regularization strategy

Perzyna model (1966) - (in cooperation with Maria Lazari)

$$\dot{\sigma} = D^{el} : \left(\dot{\varepsilon} - \dot{\varepsilon}^{vp} \right) \qquad \dot{\varepsilon} = \dot{\varepsilon}^{el} + \dot{\varepsilon}^{vp} \qquad \dot{\boldsymbol{\varepsilon}}^{\mathbf{vp}} = \lambda \frac{\partial Q}{\partial \sigma} \quad \text{where} \quad \lambda = \gamma \left\langle \varphi\left(\frac{F}{F_0} \right) \right\rangle$$

F_0: is a reference fixed value making F/F_0 dimensionless,

γ: is a "fluidity" parameter, depends on the viscosity (η) of the material and can be constant (γ=1/η) or a function of the stress or strain rate.

"<·>" are the McCauley brackets, such that: $\langle \varphi(x) \rangle = \begin{cases} \varphi(x) & \text{if } \varphi(x) \geq 0 \\ 0 & \text{if } \varphi(x) < 0 \end{cases}$

MUMOLADE

Strain localization in globally undrained dense sand

Visco-plasticity as regularization strategy

Drucker-Prager visco-plasticity, Perzyna model (1966)

(in cooperation with Maria Lazari)

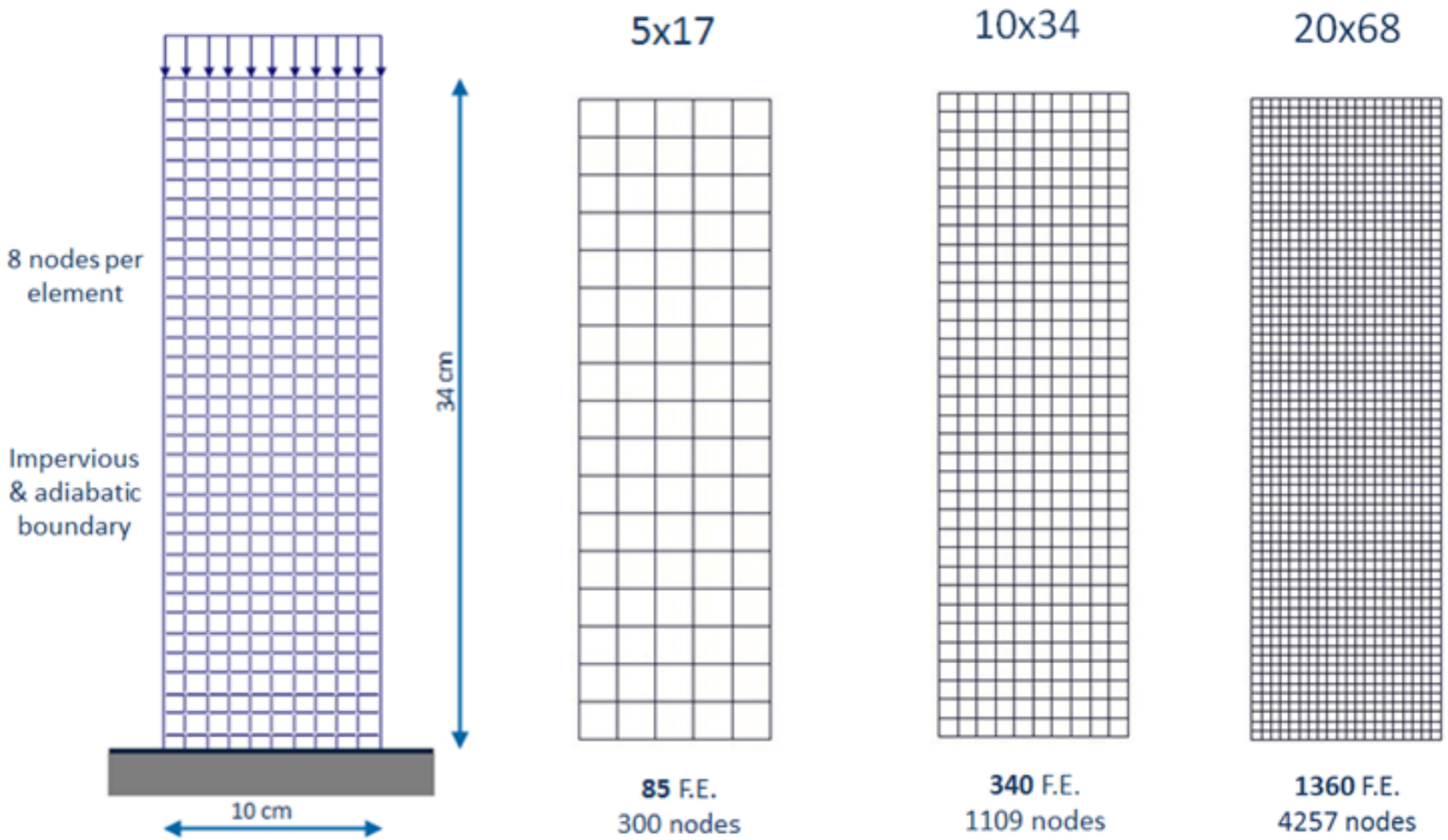

Strain localization in globally undrained dense sand

Drucker-Prager visco-plasticity – Perzyna formulation

Loading velocity:1.2mm/s

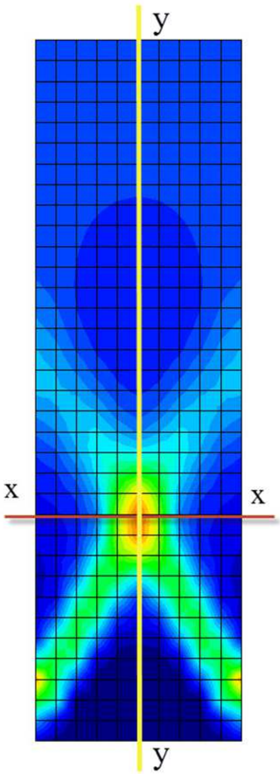

Viscosity, η=20 sec

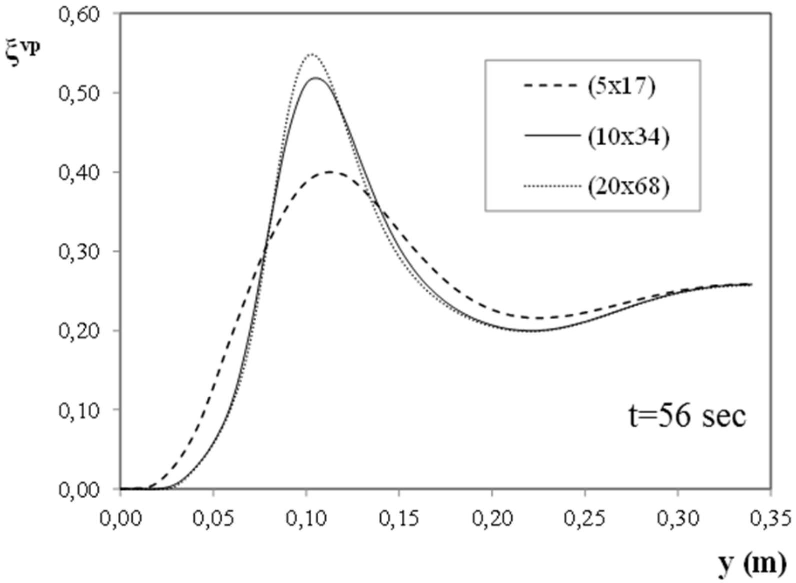

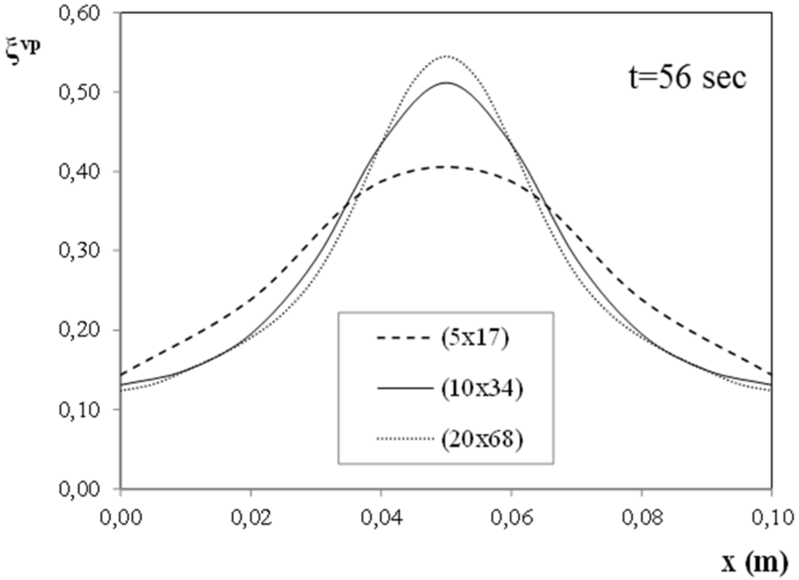

Viscosity, η=30 sec

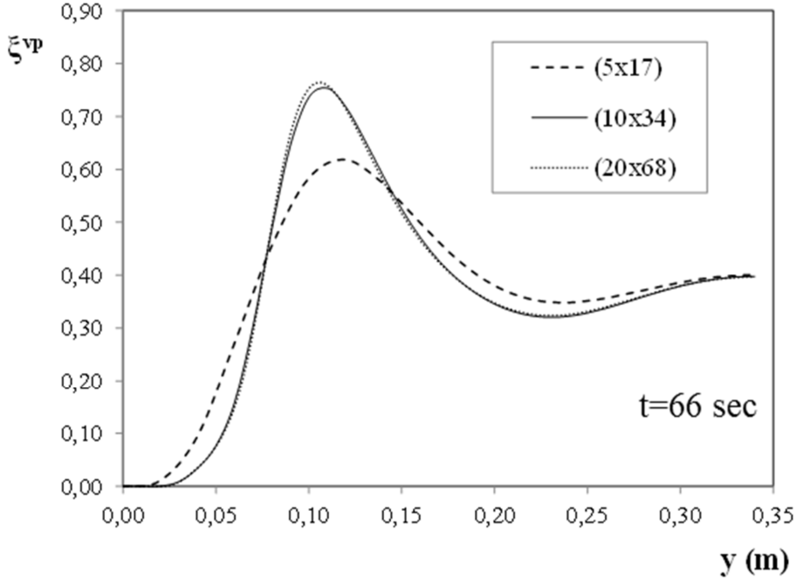

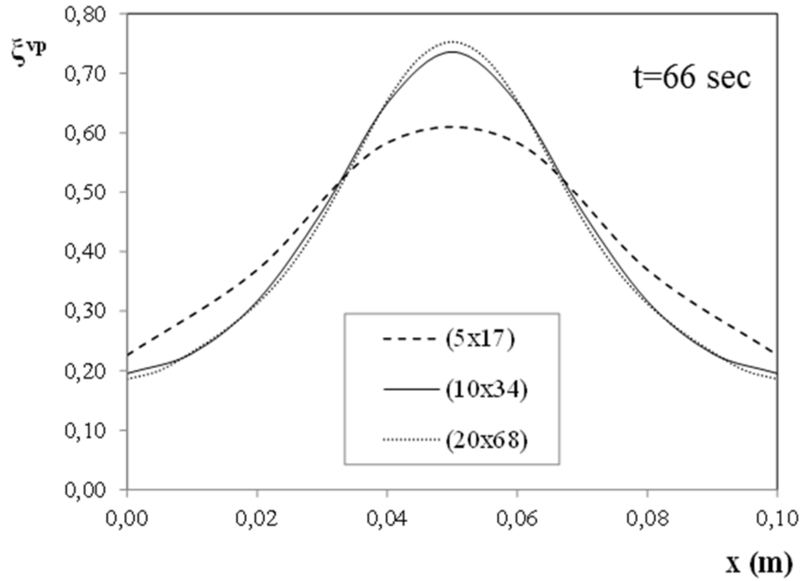

Equivalent viscoplastic strain at the horizontal (y=0,1 m) and vertical middle section of the sample

Concluding remarks

• Presented a fully coupled THM model for non-isothermal elasto-plastic variably saturated porous materials in dynamics

• Novel contribution: u-p-T formulation (for low frequencies problems)

• Model implemented in Come-geo code (University of Padova, Italy)

• Validation steps

• Dynamic strain localisation in globally undrained dense sand including frictional heating and a test case of rapid landslide have been presented

Perspectives

• Extension to non-local visco-plasticity - Implementation of Nova-diPrisco-Buscarnera model for sand - Parallel solution and 3D model

• Application to real cases (e.g. catastrophic landslides)

Some references (from my work; see also https://www.researchgate.net/profile/Lorenzo_Sanavia)

- Cao T.D., L. Sanavia, B.A. Schrefler, A thermo-hydro-mechanical model for multiphase geomaterials in dynamics with application to strain localization simulation, International Journal for Numerical Methods in Engineering (in review).
- Lazari M., L. Sanavia, B.A. Schrefler (2015), Local and non-local elasto-viscoplasticity in strain localization analysis of multiphase geomaterials, International Journal for Numerical and Analytical Methods in Geomechanics. 39, 1570-1592.
- Gawin D., L. Sanavia (2010), Simulation of cavitation in water saturated porous media considering effects of dissolved air. Transport in porous media, 81, 141-160. 2010.
- Gawin D., Sanavia L. (2009) A unified approach to numerical modelling of fully and partially saturated porous materials by considering air dissolved in water. Computer Modeling in Engineering & Sciences, 53(3), 255-302.
- Sanavia L. (2009) Numerical Modelling of a Slope Stability Test by Means of Porous Media Mechanics, Engineering Computations, 26(3), 245-266.
- Sanavia L., B. François, R. Bortolotto, L. Luison, L. Laloui (2008) Finite element modelling of thermo-elasto-plastic water saturated porous materials, Journal of Theoretical and Applied Mechanics 38(1-2), 7-24. ISSN: 0861-6663. http://www.imbm.bas.bg/tm/jtam/vol.38-1-2.php
- Cola S., L. Sanavia, P. Simonini, B.A. Schrefler (2008) Coupled thermo-hydro-mechanical analysis of Venice lagoon marshes. Water Resources Research, 44, W00C05, 16 pp. ISSN: 0043-1397. DOI:10.1029/2007WR006570.
- Zhang H.W., Qin J.M., Sanavia L., Schrefler B.A. (2007) Some theoretical aspects of strain localization analysis of multiphase porous media with regularized constitutive models, Mechanics of Advanced Materials and Structures14(2), 107-130. DOI: 10.1080/15376490600688771.
- Schrefler B.A., Zhang H.W., Sanavia L. (2006) Interaction between different internal length scales in fully and partially saturated porous media – The 1-D case, International J. for Numerical and Analytical Methods in Geomechanics, 30, 45-70. DOI:10.1002/nag.474.
- Sanavia L., F. Pesavento, B.A. Schrefler (2006) Finite element analysis of non-isothermal multiphase geomaterials with application to strain localisation simulation, Computational Mechanics, 37 (4), 331-348. DOI 10.1007/s00466-005-0673-6.
- Sanavia L., F. Pesavento, B.A. Schrefler (2005) Finite element analysis of strain localization in multiphase materials, Revue européenne de genie civil, 9, (5-6), 767-778 (European Journal of Environmental and Civil Engineering). ISSN: 1774-7120. ISBN: 2-7462-1271-4. DOI: 10.1080/17747120.2005.9692781.

- Sanavia L., B.A. Schrefler (2002) A finite element model for water saturated and partially saturated geomaterials, Revue française de genie civil (European Journal of Environmental and Civil Engineering), 6, 1083-1098. ISSN: 1279-5119. ISBN: 2-7462-0537-8. DOI: 10.1080/12795119.2002.9692733.
- Schrefler B.A., L. Sanavia (2002) Coupling equations for water saturated and partially saturated geomaterials, Revue française de genie civil (European Journal of Environmental and Civil Engineering), 6, 975-990. ISSN: 1279-5119. ISBN: 2-7462-0537-8. DOI: 10.1080/12795119.2002.9692727.
- Sanavia L., B.A. Schrefler, P. Steinmann (2002) A formulation for an unsaturated porous medium undergoing large inelastic strains, Computational Mechanics, 28, (2), 137-151.
- Zhang H.W., Sanavia L., Schrefler B.A. (2001) Numerical analysis of dynamic strain localisation in initially water saturated dense sand with a modified generalised plasticity model. Computers and Structures, 79, 441-459.
- Schrefler B.A., Zhang H.W., Sanavia L. (1999) Fluid-structure interaction in the localisation of Saturated porous media, ZAMM Zeitschrift für Angewandte Mathematik und Mechanik (Journal of Applied Mathematics and Mechanics, Z. Angew. Math. Mech.), 79, (7), 481-484. ISSN: 0044-2267, DOI: 10.1002/(SICI)1521-4001(199907)79:7<481::AID-ZAMM481>3.0.CO;2-B.
- Zhang H.W., Sanavia L., Schrefler B.A. (1999) An internal length scale in dynamic strain localisation of multiphase porous media, International J. Mechanics of Cohesive-Frictional Materials, 4, 443-460.
- Gawin D., Sanavia L., Schrefler B.A. (1998) Cavitation modelling in saturated geomaterials with application to dynamic strain localisation, International J. for Numerical Methods in Fluids, 27, 1998, 27(1-4) 109-125. DOI: 10.1002/(SICI)1097-0363(199801)27:1/4<109::AID-FLD653>3.0.CO;2-M.
- Schrefler B.A., Sanavia L., Majorana C.E. (1996) A multiphase medium model for localization and post localization simulation in geomaterials, Mechanics of Cohesive-Frictional Materials, 1, 95-114. DOI: 10.1002/(SICI)1099-1484(199601)1:1<95::AID-CFM5>3.0.CO;2-D.
- Schrefler B.A., Majorana C.E., Sanavia L. (1995) Shear band localization in saturated porous media, Archives of Mechanics, 47(3), 577-599. ISSN 00373-2029. 2004